AD 749088

Development of a Concept for a High Capacity Pneumatic Conveying System Employing a Fluid Attachment Device for Use in Underground Excavation

Semiannual Technical Report
August 30, 1972

U.S. Bureau of Mines
Contract Number H0220027

Sponsored by
Advanced Research Products Agency
ARPA Order 1579, Amendment 3
Program Code 62701D

D D C
RECEIVED
SEP 28 1972
B

The views and conclusions contained in this document are those of the authors and should not be interpreted as necessarily representing the official policies, either expressed or implied, of the Advance Research Projects Agency or the U.S. Government.

Reproduced by
NATIONAL TECHNICAL
INFORMATION SERVICE
U S Department of Commerce
Springfield VA 22151

Battelle
Pacific Northwest Laboratories
Richland, Washington 99352

DISTRIBUTION STATEMENT A
Approved for public release;
Distribution Unlimited

52

UNCLASSIFIED
Security Classification

3200.8 (Att 1 to Encl 1)
Mar 7, 66

DOCUMENT CONTROL DATA - R & D

(Security classification of title, body of abstract and indexing annotation must be entered when the overall report is classified)

1. ORIGINATING ACTIVITY (Corporate author)
Pacific Northwest Laboratories a Division of Battelle Memorial Institute

2a. REPORT SECURITY CLASSIFICATION
Unclassified

2b. GROUP

3. REPORT TITLE
Development of a concept for a High Capacity Pneumatic Conveying System Employing a Fluid Attachment Device for Use in Underground Excavation

4. DESCRIPTIVE NOTES (Type of report and inclusive dates)
Semiannual Report

5. AUTHOR(S) (First name, middle initial, last name)

6. REPORT DATE
August 30, 1972

7a. TOTAL NO. OF PAGES
50

7b. NO. OF REFS
8

8a. CONTRACT OR GRANT NO.
H0220027

b. PROJECT NO.

c.

d.

9a. ORIGINATOR'S REPORT NUMBER(S)
None

9b. OTHER REPORT NO(S) (Any other numbers that may be assigned this report)
None

10. DISTRIBUTION STATEMENT
Distribution of this document is unlimited.

11. SUPPLEMENTARY NOTES

12. SPONSORING MILITARY ACTIVITY
Advanced Research Projects Agency
Washington, D.C. 20301

13. ABSTRACT

A 12-month program with the objective to develop a mathematical model of fluid flow in Coanda eductors is about 50% complete. The model is to serve as a tool in design of Coanda eductors for pneumatic conveying of excavated rock materials. Based on work completed, it has been concluded that Coanda eductors possess potential advantages compared to alternate ejectors or other momentum transfer devices. The advantages are primarily related to the simplicity of the mechanical design. A review of literature has shown that very little information is available concerning the fluid mechanics of the Coanda eductor, the needed information will have to be developed as part of the present program. Of the alternate mathematical approaches available, one based on application of an existing fluid mechanics code was considered the most desirable, and continuing work will be keyed to this mathematical approach. Ongoing work includes development of the fluid mechanics code, and experimental measurements of flow fields in model eductors which will provide input data for the model and serve as a basis for evaluating model predictions.

DD FORM 1 NOV 65 1473

UNCLASSIFIED
Security Classification

14 KEY WORDS	LINK A ROLE	LINK A WT	LINK B ROLE	LINK B WT	LINK C ROLE	LINK C WT
Coanda Effect						
Wall Jet						
Eductor						
Pneumatic Conveying						
Fluid Mechanics						
Numerical Computer Code						
Navier-Stokes Equations						
Underground Excavation						

SEMIANNUAL TECHNICAL REPORT
COVERING TECHNICAL WORK FROM
FEBRUARY 10, 1972 TO AUGUST 10, 1972

ARPA Order Number: 1579, Amendment 3

Program Code Number: 62701D

Name of Contractor:

Pacific Northwest Laboratories
a division of Battelle Memorial
Institute

Effective Date of Contract:

February 10, 1972

Contract Expiration Date:

April 10, 1973

Amount of Contract:

$74,820

Contract Number:
H0220027

Program Director*

D. E. Rasmussen

Telephone Number: (509) 946-2407

Short Title of Work:

Development of a Concept for a High Capacity Pneumatic Conveying System Employing a Fluid Attachment Device for Use in Underground Excavation

This research was supported by the Advanced Research Projects Agency of the Department of Defense and was monitored by Bureau of Mines under Contract Number H0220027.

* For project functional organization, see Appendix A.

FOREWORD

This report summarizes the first six months work completed by Battelle-Northwest for the U.S. Bureau of Mines under Contract Number H0220027. The program director is D. E. Rasmussen and principal investigators are A. K. Postma, J. D. Smith and D. S. Trent.

TABLE OF CONTENTS

	Page
FOREWORD	ii
LIST OF FIGURES	iv
INTRODUCTION	1
SUMMARY	2
CONCLUSIONS AND RECOMMENDATIONS	3
LITERATURE REVIEW	4
MATHEMATICAL MODEL DEVELOPMENT	10
DIFFERENTIAL EQUATIONS OF FLUID FLOW	11
DIMENSIONAL ANALYSIS	15
SIMILARITY THEORY	18
NUMERICAL MODEL BASED ON VORTICITY TRANSPORT THEORY	20
Mathematical Basis	20
Vorticity Transport	22
Description of the SYMJET Code (Coanda Version)	24
Application of the SYMJET Code to the Coanda Eductor	30
EXPERIMENTAL PROGRAM	35
REFERENCES	37
APPENDIX A - PROJECT ORGANIZATION CHART	A.1
APPENDIX B - BIBLIOGRAPHY	B.1
DISTRIBUTION	Distr-1

LIST OF FIGURES

		Page
1	Results of Bourque and Newman[1] for Attachment of Plane Jet to Inclined Plane	6
2	Results of Sridhar and Tu[2] for Dimensionless Entrainment as a Function of Surface Curvature	7
3	Cross Section of Cylindrical Eductors	8
4	Air Ejector Performance for Motive Air Supply Pressures	9
5	Schematic View of Hypothetical Coanda Eductor Showing Geometric Parameters	17
6	Typical Finite Difference Cell Illustrating Indices for Ψ, ω, and V.	27
7	Calculational Grid System Showing Boundary Conditions and Grid Spacing	31
8	Streamlines Predicted for an Entrainment Ratio of 5.	33
9	Streamlines Predicted for an Entrainment Ratio of 0.8.	34
10	Schematic View of Experimental Equipment	36

DEVELOPMENT OF A CONCEPT FOR A HIGH CAPACITY
PNEUMATIC CONVEYING SYSTEM EMPLOYING A FLUID ATTACHMENT DEVICE
FOR USE IN UNDERGROUND EXCAVATION

to

U.S. BUREAU OF MINES

CONTRACT NUMBER H0220027

INTRODUCTION

This report describes the work completed during the first six months of a program being carried out by Battelle-Northwest for the U.S. Bureau of Mines. The objective of this research program is to develop a mathematical model to describe the fluid mechanics of a Coanda eductor. A satisfactory model will serve as a tool in design of Coanda eductors for pneumatic conveying of excavated rock materials. The report includes a summary of work accomplished, conclusions and recommendations, followed by detailed discussions presented in sections entitled Literature Review, Mathematical Model Development and Experimental Program.

The possible use of a Coanda eductor for pneumatic transport was suggested by preliminary experiments carried out at Battelle-Northwest. A small model was found to be highly effective in entraining granular materials and discussions with personnel from the U.S. Bureau of Mines led to the current interest in assessing the potential use of such an eductor in transporting rock in underground excavations.

The term "Coanda" derives from the Romanian-born engineer named Henri Coanda. Henri Coanda nearly suffered an early demise as a result of unexpected flow along exhaust deflector plates he had installed on a wooden airplane powered by a type of jet engine. Instead of deflecting the exhaust gas away from the wooden fuselage, installed deflector plates were actually sucking the flames toward it. Coanda survived this mishap, and spent much of the remainder of his life studying the curious attachment phenomena which accompany flow along solid surfaces. Most of the scientific effort devoted to attached or "Coanda" flow has been directed to the use of the phenomenon in vehicle propulsion.

Use of the fluid attachment principle in an eductor is attractive because of very simple mechanical designs which are possible, and more importantly, because of the possibility of designing eductors with large throat openings free from obstructions. These advantages are of potentially great importance in pneumatic conveying of solids. This problem had not been studied previously to an appreciable extent. The approach taken in the present study is to develop a mathematical model which adequately describes fluid flow in Coanda eductors. The merits for using a Coanda eductor in a specific case can then be judged from eductors designed to meet specific requirements of flow rate and pressure drop.

SUMMARY

A 12-month program with the objective to develop a mathematical model of fluid flow in Coanda eductors is about 50% complete. Tasks which have been completed include writing a detailed program plan, reviewing available technical literature, and making a comparison of performance of Coanda eductors with other momentum transfer methods. Ongoing work includes development of a numerical computer program for solving the differential equation of fluid flow for axial symmetric flow, and experimental measurements of flow fields in model eductors.

Many studies of wall jet flow have been performed for two-dimensional flow over flat and curved surfaces. The experimental and theoretical data that are available, however, do not apply directly to flow in cylindrical, axisymmetric geometries of interest for the Coanda eductor.

Comparison of the Coanda eductor with other types of momentum transfer devices indicated that the chief advantages offered by this eductor lie in its extreme mechanical simplicity, and in its large open throat. Energy requirements for the Coanda eductor are expected to be higher than for mechanical systems such as conveyers or airlock feeders. Energy requirements are expected to be equivalent to those for presently available ejectors.

Three approaches to building a mathematical model for the flow field were considered. These included model theory based on dimensional analysis, similarity theory, and numerical solution of the complete Navier-Stoakes equations. A decision was made to pursue the latter approach because it can provide the most detailed description of the flow field with the least amount of experimental data. An existing computer code which solves the Navier-Stokes equations for flows having axial symmetry was modified to calculate the flow field for a Coanda eductor. To the present, steady-state, well converged solutions have been obtained using a computational grid with 1200 nodes. Effort in the immediate future will concentrate on solution of the pressure equation and on means for realistically handling eddy viscosities.

An experimental apparatus has been designed to provide data on pressure drop, entrained flow, and velocity profiles for several geometries. The experimental data will be used to test the validity of the mathematical model and to provide input regarding numerical values of eddy viscosity.

CONCLUSIONS AND RECOMMENDATIONS

The work completed to date supports the following conclusions:

- The Coanda eductors possess potential advantages compared to alternate ejectors or other momentum transfer devices. The advantages are primarily related to the simplicity of the mechanical design.
- Very little quantitative information is available concerning the fluid mechanics of the Coanda eductor. The needed information will have to be developed.
- Of the alternate mathematical approaches available, the one based on an existing fluid mechanics code is the most desirable.
- This effort should be continued to develop the information base needed to design Coanda eductors for underground excavation applications.

LITERATURE REVIEW

Literature on the Coanda effect was reviewed with the purpose of gathering information which would support the present Coanda eductor study. A bibliography of the literature reviewed is included as Appendix B. The review revealed that very little information is available concerning wall jet behavior in geometries with cylindrical symmetry. A number of studies, both theoretical and experimental, have dealt with two-dimensional flow over flat and curved surfaces. In addition, a relatively large body of information has been developed for ejectors (or jet pumps) which entrain fluid by flowing primary air through a tube centered in a larger mixing tube. For the Coanda eductor, the primary air is introduced through an annular slit, and becomes attached to the inlet surface prior to entry into a mixing zone. Geometries for the two eductors are similar downstream from the entry to mixing section, hence information developed for this region in ejectors should apply to the Coanda eductor. The following paragraphs briefly describe the information obtained from the literature search.

Studies of ejectors have included both theoretical and experimental approaches. Theoretical studies consist of the one-dimensional approach, with details of the fluid mechanics typically being neglected. Reversible thermodynamics have been assumed along with equations of state for the fluids. Thus, the theoretical analyses establish an upper limit to performance, but shed little light on how to design Coanda eductors to achieve the maximum performance. Experimental studies with air ejectors have shown optimum designs. The length-to-diameter ratio for the mixing section is found to be near 7. The optimum angle of divergence in the outlet diffuser is found to be in the 7° to 10° range. Because of the similarity in geometry, these optimum parameters would be expected to apply to the Coanda eductor.

Attachment of air jets to surfaces has been the subject of a number of experimental studies. Applications have been directed primarily

toward fluidic amplifiers and to aircraft propulsion. Jet attachment has been studied as a function of jet width, step height, and angle of inclination of attachment surface compared to the slit. From the results one can predict the distance of attachment as a function of these conditions. Several studies have focused on the effect of curvature on detachment and fluid entrainment. Entrainment increases with increasing curvature where curvature is defined as the reciprocal of the radius of curvature (1/R). From these results, one would expect that the greatest entrainment ratios could be obtained by using large curvature upstream from the constant area mixing section of the Coanda eductor. On the other hand, the largest pressures could likely be developed using inlet surfaces which employed less curvature.

To date, the most realistic theoretical approaches have relied on similarity theory to simplify the flow equations, thus permitting solution. This similarity approach appears to be quite successful in predicting the flow field for flat and curved two-dimensional flows. Similarity has not been applied to the axisymmetric case of interest in the Coanda eductor.

Several examples of reported results are briefly discussed here. Figure 1 shows the results of Bourque and Newman[1] for reattachment of a jet to an inclined plane. The minimum length of plate required to cause spontaneous attachment is shown as the upper curve. The maximum angle at which spontaneous attachment occurs is approximately 50°. Once the jet becomes attached, however, a hysteresis effect becomes evident since attachment can be maintained up to about 65°.

Experimental data on entrainment for jet flow along the surface of a cylinder were reported by Sridhar and Tu.[2] Their results are shown in Figure 2, in which the dimensionless entrainment velocity is shown as a function of curvature of the cylindrical surface. For convex surfaces, entrainment per unit length increases as the radius of curvature decreases. For convex surfaces, just the opposite occurs.

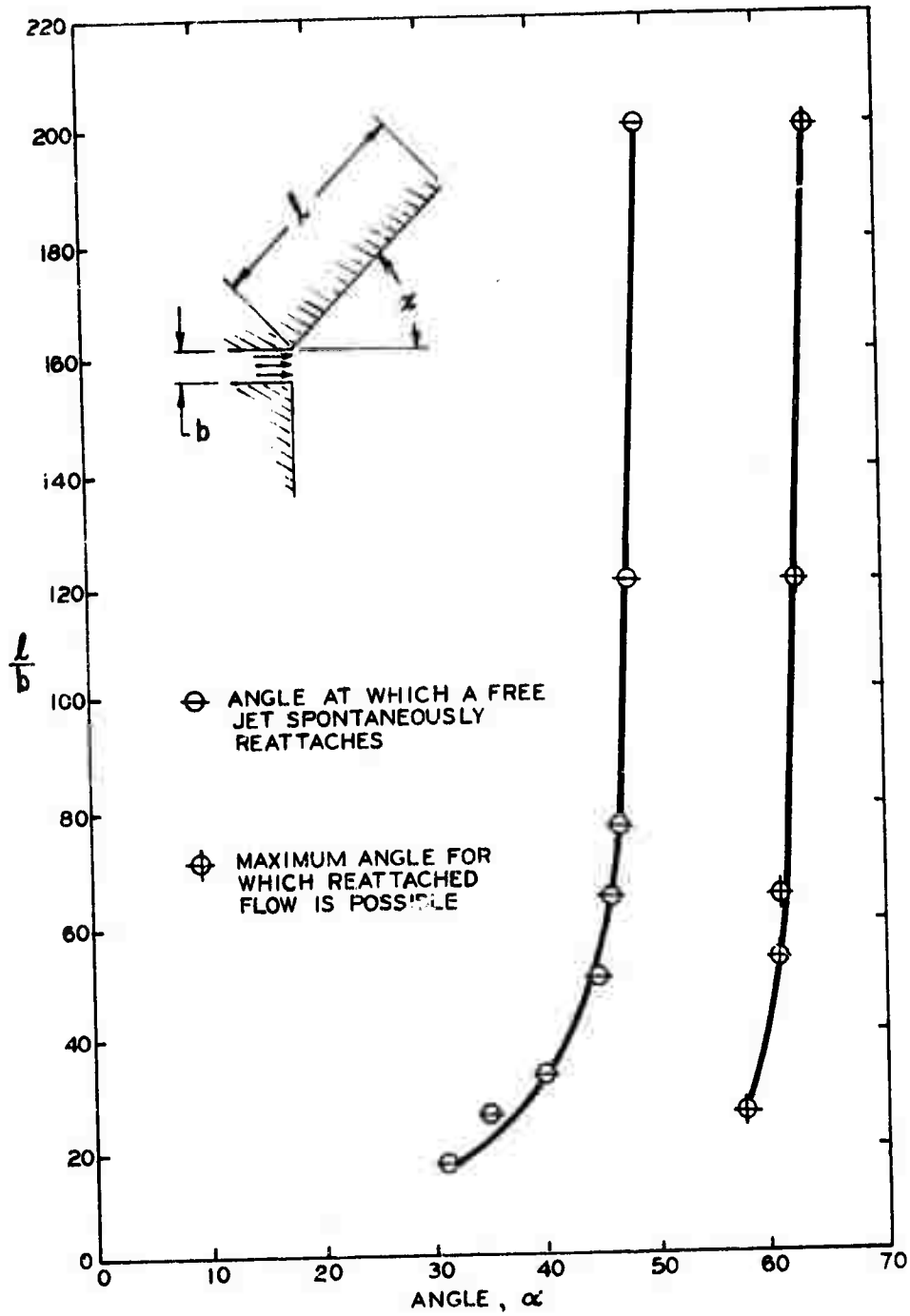

FIGURE 1. Results of Bourque and Newman[1] for Attachment of Plane Jet to Inclined Plane

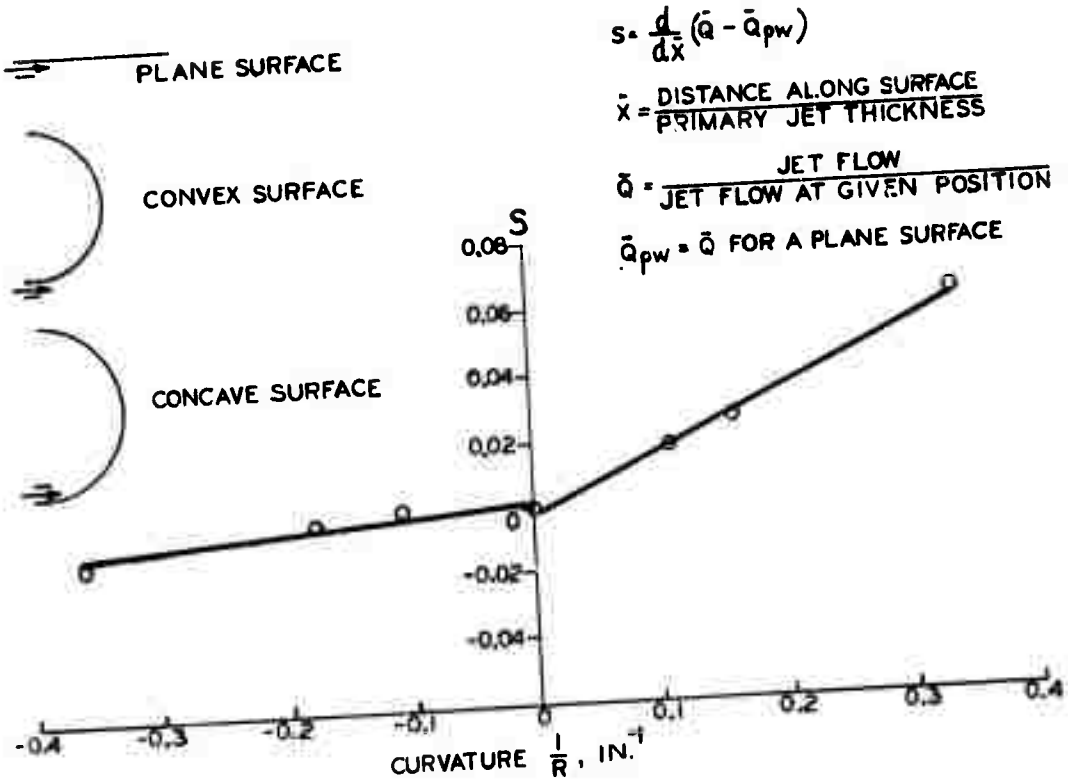

FIGURE 2. Results of Sridhar and Tu[2] for Dimensionless Entrainment as a Function of Surface Curvature

The literature review was primarily concerned with studies conducted on the "Coanda effect" and on "wall jets". Some of the material was useful in our effort to develop a reliable analytical method for the design of eductors incorporating the fluid attachment principle. However, little was revealed that would provide the basis for a reliable comparison of a Coanda eductor to other momentum transfer methods. It is, however, reasonable to assume that the performance of a Coanda eductor will be similar to that of an air ejector since both incorporate inlet entrainment regions for a high velocity motive jet to entrain ambient air, a constant cross-sectional area mixing region, and a diffusor section to increase the discharge pressure (see Figure 3). If this assumption is valid, then from air ejector technology we can predict the performance for Coanda eductors. Figure 4 shows anticipated performance for a family of motive air supply pressures in terms of entrainment (R_W) and discharge pressure.

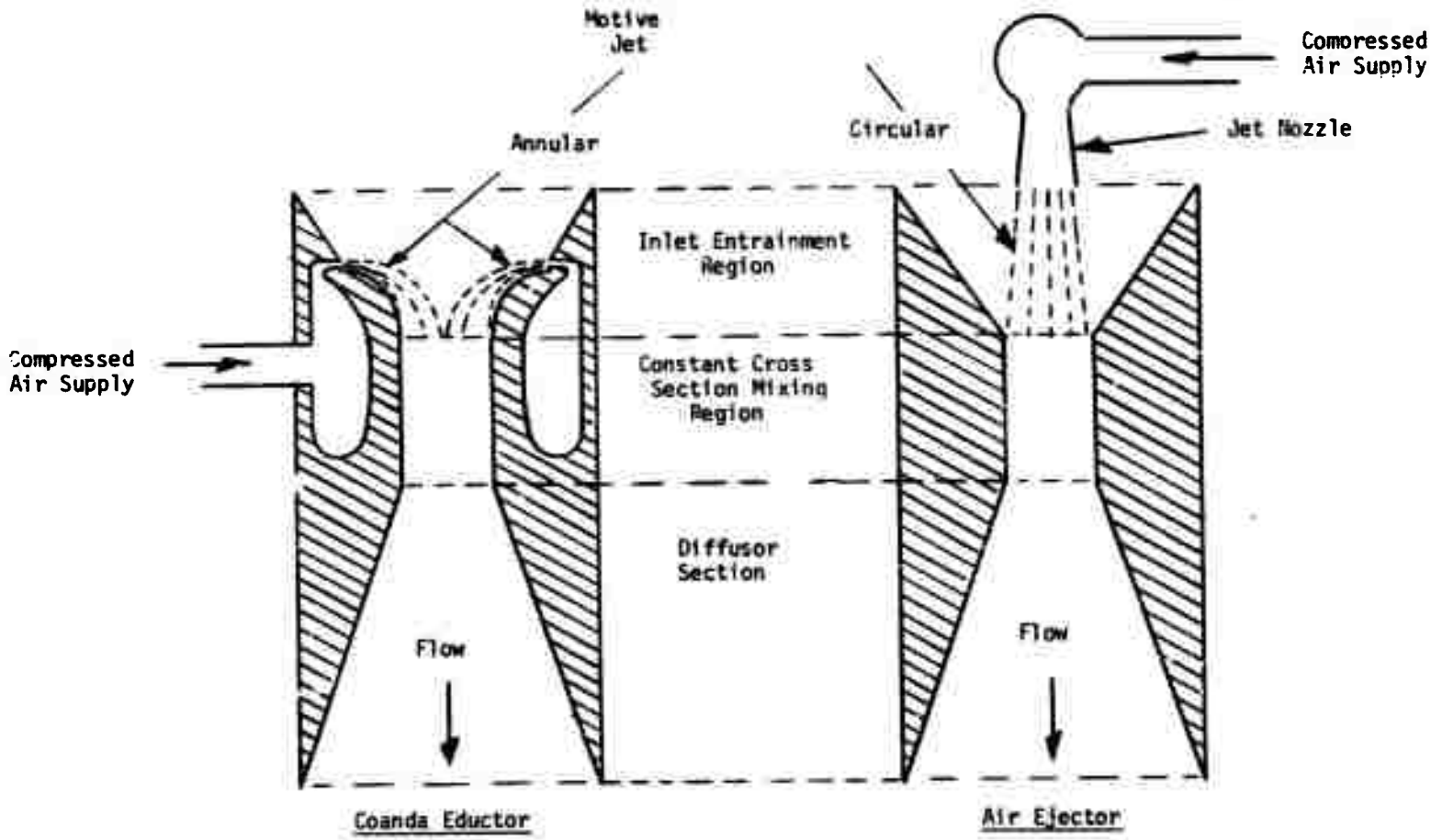

FIGURE 3. Cross Section of Cylindrical Eductors

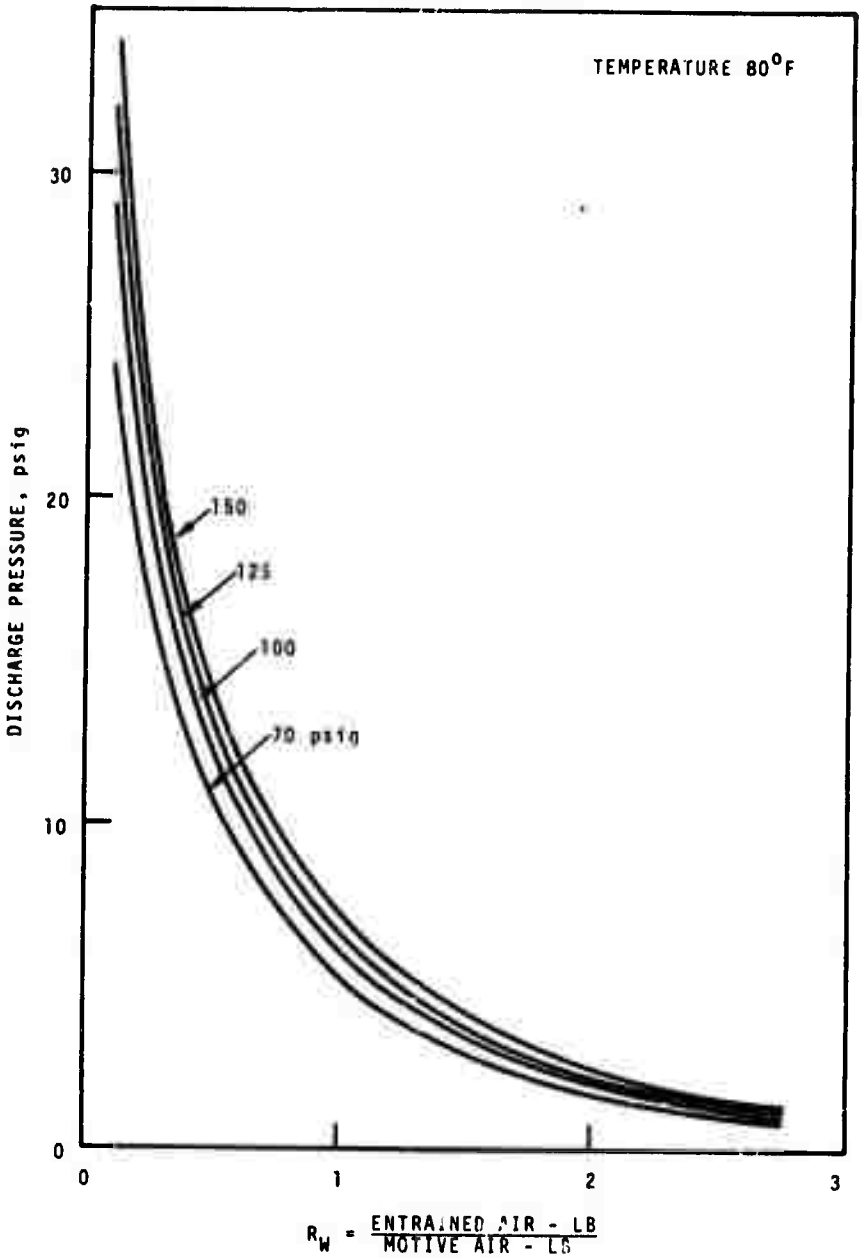

FIGURE 4. Air Ejector Performance for Motive Air Supply Pressures

MATHEMATICAL MODEL DEVELOPMENT

The ultimate use of the mathematical model will be to predict material transport rates for eductors employing the Coanda effect. The material transport capabilities of the eductor are expected to be related closely to the air flow rate and the pressure drop developed across the eductors. Thus, the mathematical model should permit prediction of these two parameters as a function of design elements including fluid properties, primary jet velocity, and geometric design of a specific eductor.

To develop a theoretical model within the time allotted, we identified three possible approaches. The first approach was to use model theory which relies on dimensional analysis to permit scaling of data from model to prototype. The second approach was to use similarity theory. This involves simplifying assumptions to convert boundary layer partial differential equations to total differential equations which are easily solved. Similarity theory has been used successfully in modeling wall jet flows.[3] The third potential theoretical approach involved adapting an existing fluid flow computer code capable of numerically solving the Navier-Stokes equations for axial symmetric flow fields.

Our first efforts were to briefly survey these theoretical approaches to verify the plausibility of each for application to the present problem. The second step effort was concentrated on the use of an existing numerical computer code since it promised the most accurate prediction of the flow field and also because it requires the least amount of experimental data as input. At present we have experienced some success in applying the computer program; thus, we are continuing to concentrate on this approach. If the numerical approach continues to prove promising, no additional effort will be devoted to the other two alternates. Each of the three alternative mathematical approaches is described further in the following sections of this report.

DIFFERENTIAL EQUATIONS OF FLUID FLOW

The mathematical formulation of the differential equations for fluid flow are obtained by making mass, force, and energy balances on a small fluid element in space. These basic equations form the basis for theoretical attacks on the fluid flow problem. Although the full set of equations is too complicated to solve generally, they were listed to establish the following:

- Simplifying assumptions used in various theoretical approaches
- Identification of important physical parameters
- Description of important boundary conditions
- Basis for dimensional analysis.

The continuity equation results from a statement that mass is conserved. For cylindrical coordinates, the continuity equation is

$$\frac{\partial \rho}{\partial t} + \frac{1}{r}\frac{\partial}{\partial r}\left(\rho r v_r\right) + \frac{1}{r}\frac{\partial}{\partial \theta}\left(\rho v_\theta\right) + \frac{\partial}{\partial z}\left(\rho v_z\right) = 0 \qquad (1)$$

where

ρ = fluid density,
t = time
r = distance measured in radial direction,
v_r = fluid velocity in radial direction,
v_θ = fluid velocity in θ direction,
v_z = fluid velocity in z direction,
θ = angular position measured around z axis,
z = distance measured in axial direction.

As written, Equation (1) applies to the three-dimensional flow of a compressible fluid. For special cases, this equation may be appreciably simplified.

The momentum equations are derived by balancing the forces on a fluid element. Statically unbalanced forces are equated to the fluid mass

times its acceleration. Thus, it amounts to application of Newton's second law of motion to a small fluid element. However, deformation of the fluid element by tangential forces must also be accounted for, and this greatly complicates the equations of motion as compared to those for nondeformable bodies. For three-dimensional flow, three separate momentum equations result. Written in cylindrical coordinates, in terms of stress components, the momentum equations are as follows:

r-component
$$\rho\left(\frac{\partial v_r}{\partial t} + v_r \frac{\partial v_r}{\partial r} + \frac{v_\theta}{r}\frac{\partial v_r}{\partial \theta} - \frac{v_\theta^2}{r} + v_z \frac{\partial v_r}{\partial z}\right) = -\frac{\partial p}{\partial r}$$

$$-\left[\frac{1}{r}\frac{\partial}{\partial r}\left(r\tau_{rr}\right) + \frac{1}{r}\frac{\partial \tau_{r\theta}}{\partial \theta} - \frac{\tau_{\theta\theta}}{r} + \frac{\partial \tau_{rz}}{\partial z}\right] + \rho g_r \qquad (2)$$

θ-component
$$\rho\left(\frac{\partial v_\theta}{\partial t} + v_r \frac{\partial v_\theta}{\partial r} + \frac{v_\theta}{r}\frac{\partial v_\theta}{\partial \theta} + \frac{v_r v_\theta}{r} + v_z \frac{\partial v_\theta}{\partial z}\right) = -\frac{1}{r}\frac{\partial p}{\partial \theta}$$

$$-\left[\frac{1}{r^2}\frac{\partial}{\partial r}\left(r^2\tau_{r\theta}\right) + \frac{1}{r}\frac{\partial \tau_{\theta\theta}}{\partial \theta} + \frac{\partial \tau_{\theta z}}{\partial z}\right] + \rho g_\theta \qquad (3)$$

z-component
$$\rho\left(\frac{\partial v_z}{\partial t} + v_r \frac{\partial v_z}{\partial r} + \frac{v_\theta}{r}\frac{\partial v_z}{\partial \theta} + v_z \frac{\partial v_z}{\partial z}\right) = -\frac{\partial p}{\partial z}$$

$$-\left[\frac{1}{r}\frac{\partial}{\partial r}\left(r\tau_{rz}\right) + \frac{1}{r}\frac{\partial \tau_{\theta z}}{\partial \theta} + \frac{\partial \tau_{zz}}{\partial z}\right] + \rho g_z \qquad (4)$$

These momentum equations apply quite generally because simplifying assumptions have not yet been made.

The energy equation is obtained from an energy balance written on a small fluid element. In cylindrical coordinates it may be written in terms of stress components as

$$\rho\hat{C}_v\left(\frac{\partial T}{\partial t} + v_r\frac{\partial T}{\partial r} + \frac{v_\theta}{r}\frac{\partial T}{\partial \theta} + v_z\frac{\partial T}{\partial z}\right) = -\left[\frac{1}{r}\frac{\partial}{\partial r}\left(rq_r\right) + \frac{1}{r}\frac{\partial q_\theta}{\partial \theta} + \frac{\partial q_z}{\partial z}\right]$$

$$- T\left(\frac{\partial P}{\partial T}\right)_\rho\left[\frac{1}{r}\frac{\partial}{\partial r}\left(rv_r\right) + \frac{1}{r}\frac{\partial v_\theta}{\partial \theta} + \frac{\partial v_z}{\partial z}\right] - \left[\tau_{rr}\frac{\partial v_r}{\partial r}\right.$$

$$\left. + \tau_{\theta\theta}\frac{1}{r}\left(\frac{\partial v_\theta}{\partial \theta} + v_r\right) + \tau_{zz}\frac{\partial v_z}{\partial z}\right] - \left\{\tau_{r\theta}\left[r\frac{\partial}{\partial r}\left(\frac{v_\theta}{r}\right) + \frac{1}{r}\frac{\partial v_r}{\partial \theta}\right]\right.$$

$$\left. + \tau_{rz}\left(\frac{\partial v_z}{\partial r} + \frac{\partial v_r}{\partial z}\right) + \tau_{\theta z}\left(\frac{1}{r}\frac{\partial v_z}{\partial \theta} + \frac{\partial v_\theta}{\partial z}\right)\right\} \tag{5}$$

where

$\hat{C}_v$ = heat capacity at constant volume,

T = temperature,

$q_r = k\frac{\partial T}{\partial r}$,

$q_\theta = -k\frac{1}{r}\frac{\partial T}{\partial \theta}$,

$q_z = -k\frac{\partial T}{\partial z}$,

k = thermal conductivity.

The stress components which are included in Equations (2) through (5) are defined as follows.

$$\tau_{rr} = -\mu\left[2\frac{\partial v_r}{\partial r} - \frac{2}{3}\left(\nabla \cdot v\right)\right]$$

$$\tau_{\theta\theta} = -\mu\left[2\left(\frac{1}{r}\frac{\partial v_\theta}{\partial \theta} + \frac{v_r}{r}\right) - \frac{2}{3}\left(\nabla \cdot v\right)\right]$$

$$\tau_{zz} = -\mu\left[2\frac{\partial v_z}{\partial z} - \frac{2}{3}\left(\nabla \cdot v\right)\right]$$

$$\tau_{r\theta} = \tau_{\theta r} = -\mu\left[r\frac{\partial}{\partial r}\left(\frac{v_\theta}{r}\right) + \frac{1}{r}\frac{\partial v_r}{\partial \theta}\right]$$

$$\tau_{\theta z} = \tau_{z\theta} = -\mu\left[\frac{\partial v_\theta}{\partial z} + \frac{1}{r}\frac{\partial v_z}{\partial \theta}\right]$$

$$\tau_{zr} = \tau_{rz} = -\mu\left[\frac{\partial v_z}{\partial r} + \frac{\partial v_r}{\partial z}\right]$$

$$\left(\nabla \cdot v\right) = \frac{1}{r}\frac{\partial}{\partial r}\left(r v_r\right) + \frac{1}{r}\frac{\partial v_\theta}{\partial \theta} + \frac{\partial v_z}{\partial z}$$

Equations (1) through (5) fully describe the flow of fluids in three-space dimension. In practice, some degree of simplification is required before these equations can be solved.

DIMENSIONAL ANALYSIS

Any mathematical relationship which is dimensionally consistent may be written as a relationship between dimensionless groups. The various techniques of dimensional analysis identify the dimensionless groups for a given physical problem. The utility of this approach is that it can greatly reduce the number of independent variables which must be considered in experiments. Once a relationship between dimensionless groups is defined by means of model experiments, predictions can be made for prototypes provided the numerical values taken by the various dimensionless groups fall within the range investigated in model tests.

One way of deriving the important dimensionless groups for a problem is based on simple mathematical operations on the basic differential equations. This method is well described by Klinkenberg and Mooy.[4] We have used this approach with the momentum and energy equations, Equations (2) through (5). The following dimensionless groups shown in Table 1 appeared from this analysis.

TABLE 1. Dimensionless Groups Obtained from Momentum and Energy Equations

Name of Dimensionless Group	Definition
Reynolds No., Re	$\rho dv/\mu$
Prandtl No., Pr	$C_p\mu/k$
Eckert No., Ec	$v^2/C_v t$
Euler No., Eu	$P/\rho v^2$
Brinkman No., Br	$\mu v^2/kT$
Specific Heat Ratio, γ	C_p/C_v
Froude No., Fr	gd/V^2

where

ρ = fluid density,

V = velocity

μ = viscosity

C_p = heat capacity at constant pressure

k = thermal conductivity

C_v = heat capacity at constant volume

T = temperature

P = pressure

g = acceleration due to gravity

d = diameter

A second approach to deriving important dimensionless groups is to list all important parameters for a given physical situation. The parameters can then be grouped as dimensionless ratios using standard techniques. A hypothetical Coanda eductor is shown schematically in Figure 5. In addition to the 12 geometric dimensions, flow properties expected to be important include: fluid density, fluid viscosity, specific heat, specific heat ratio, thermal conductivity, temperature, velocity of primary air, velocity of entrained air, and pressure drop across nozzle. Using the Buckingham method[5] for forming the dimensionless group, we obtain the following expression for the entrained air flow.

$$\frac{\text{Entrained Flow}}{\text{Primary Flow}} = \text{function (Re, Ma, Br, Eu, } \gamma\text{, geometric length ratios)} \quad (6)$$

where

Re = Reynolds No.

Ma = Mach No.

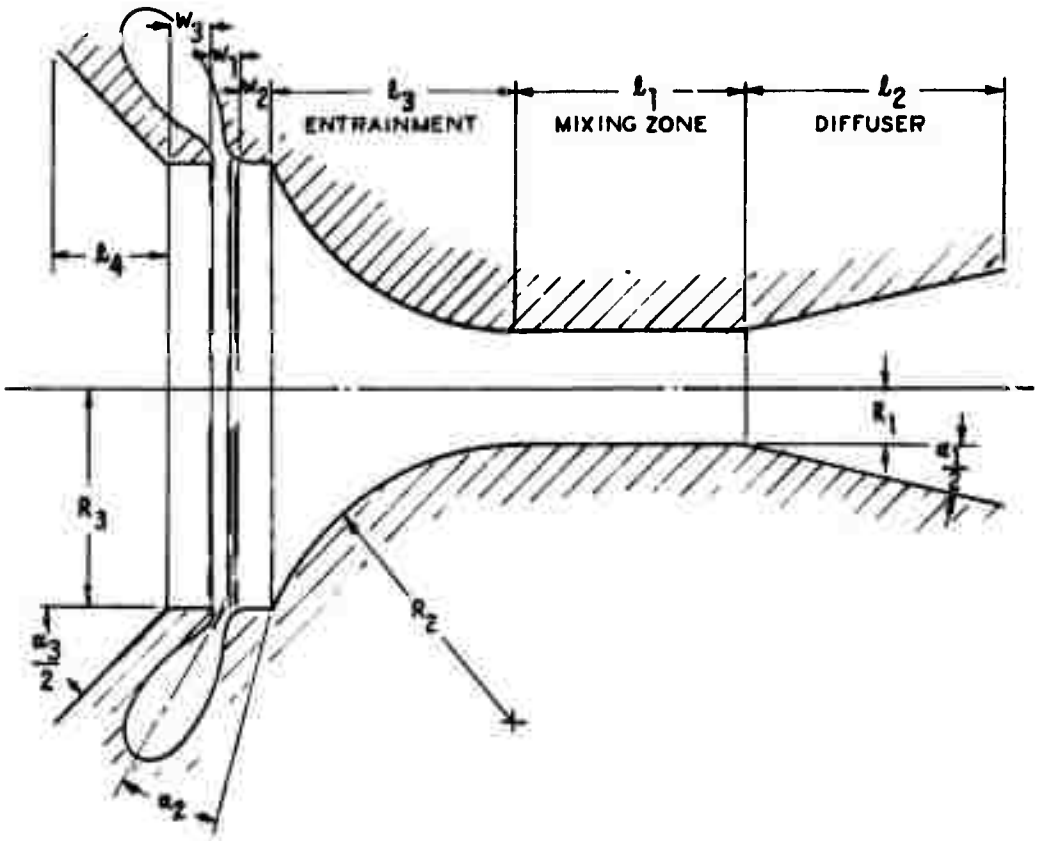

w_1 = width of primary air inlet slit

w_2 = height of step separating jet and Coanda wall

w_3 = length of inlet cylinder upstream from primary air slit

α_1 = angle of divergence of outlet diffuser

α_2 = angle of inclination of primary jet

α_3 = angle of convergence of inlet

ℓ_1 = length of mixing section (constant area)

ℓ_2 = length of outlet diffuser

ℓ_3 = length of Coanda entrainment section

ℓ_4 = length of inlet transition

R_1 = radius of throat of nozzle

R_2 = radius of curvature of Coanda entrainment section

FIGURE 5. Schematic View of Hypothetical Coanda Eductor Showing Geometric Parameter

Br = Brinkman No.

Eu = Euler No.

γ = specific heat ratio.

The Mach No. is closely related to the Eckert No. which appeared earlier. From Equation (6), one could, in theory, perform experiments that would provide the functional relationship between the groups. In practice, too many experiments would be required to evaluate the relationship among the five flow related groups and the 12 geometric ratios. The next step in using the dimensional analysis approach would be to eliminate the groups of minor importance, and key on the several controlling groups. This step was not accomplished in the present work.

SIMILARITY THEORY

Similarity theory is a method for simplifying the equations of motion to a point where they can be solved. The term "similarity" derives from the assumed shape of the velocity profile, which is assumed to have a prescribed similarity at each downstream position, x. A classical example of similarity theory is that used by Glauert[3] in his analysis of the wall jet. Glauert's beginning point is the simplified, two-dimensional boundary layer momentum equation written as

$$u \frac{\partial u}{\partial x} + v \frac{\partial u}{\partial y} = \nu \frac{\partial^2 u}{\partial y^2} \tag{7}$$

where

u = velocity in x direction,

v = velocity in y direction,

ν = kinematic viscosity.

A stream function, ψ, is defined satisfy the continuity equation:

$$-\frac{\partial\psi}{\partial x} = xv \tag{8}$$

and

$$\frac{\partial\psi}{\partial y} = xu \tag{9}$$

where

ψ = stream function.

The continuity equation may be written as

$$\frac{\partial}{\partial x}(xu) + \frac{\partial}{\partial y}(xv) = 0 \tag{10}$$

By defining a new variable, $\eta = yx^n$, the two partial differential equations, Equation (7) and Equation (10) are transformed to a total differential equation:

$$f''' + ff'' + \alpha f'^2 = 0 \tag{11}$$

In Equation (11) the argument of the function, f, is η; α is a numerical parameter related to n.

Glauert's[3] solution to Equation (11) provides velocity profiles which agree well with experimental measurements, showing that the mathematical assumptions made were justified. Presumably, similar approaches could be made for axisymmetric flows encountered in the Coanda eductor. No attempt was made to pursue the similarity theory approach, but it appears to offer potential and serves as a backup in the event the numerical approach should fail.

NUMERICAL MODEL BASED ON VORTICITY TRANSPORT THEORY

The following discusses the mathematical basis and the finite difference method of solution used in the vorticity transport method.

Mathematical Basis

The differential equations governing Coanda eductor fluid flow are derived from the two conservation laws:

- conservation of mass (continuity)
- conservation of momentum (Newton's second law).

These equations written for incompressible, turbulent flow in cartesian tensor form are:

Continuity:

$$\frac{\partial u_i}{\partial x_i} = 0 \ , \tag{12}$$

Momentum:

$$\frac{Du_i}{Dt} = -\frac{1}{\rho}\frac{\partial p}{\partial x_i} + \frac{\partial}{\partial x_j}\left(\varepsilon_{ij}\frac{\partial u_i}{\partial x_j}\right) . \tag{13}$$

In the above equations, time and spatial changes of the fluid density, ρ, have been ignored (incompressibility condition).

Notation used in Equations (12) and (13) is as follows:

u_i = velocity along i^{th} coordinate

x_i = i^{th} space coordinate

P = pressure

t = time

ε_{ij} = Eddy diffusivity tensor for momentum.

The operator D/Dt is the substantial derivative defined as

$$\frac{D}{Dt} = \frac{\partial}{\partial t} + u_j \frac{\partial}{\partial x_j}$$

The tensor index i (or j) for three-space takes values i = 1, 2 and 3. Einsteinian notation is used where a repeated index implies summation over the possible values i (or j) = 1, 2 and 3.

In the momentum Equation (13), we have neglected gravitational effects and have assumed that the effects of Reynolds stresses (turbulent stresses) may be approximated through the use of an eddy diffusivity, ε_{ij}.

For the Coanda eductor study, it is possible to express the equations of continuity and momentum in terms of axisymmetric coordinates, thus using only the two-space coordinates z (axial) and r (radial). This assumption ignores mean azimuthal variation of the dependent variables such as mean azimuthal velocity (swirl). Also, the Coanda study is directed to steady-flow operation of the eductor, hence time dependence may also be eliminated in the equations of motion.

Thus, the equations which are used for analysis of the Coanda eductor are the following steady-flow, axisymmetric equations of continuity and motion:

Continuity:

$$\frac{1}{r} \frac{\partial ur}{\partial r} + \frac{\partial v}{\partial z} = 0 \ . \tag{14}$$

Momentum:

r-direction,

$$u \frac{\partial u}{\partial r} + v \frac{\partial u}{\partial r} = - \frac{1}{\rho} \frac{\partial P}{\partial r} + \frac{\partial}{\partial r} \left(\frac{\varepsilon_r}{r} \frac{\partial ur}{\partial r} \right) + \frac{\partial}{\partial z} \left(\varepsilon_z \frac{\partial u}{\partial z} \right) , \tag{15}$$

z-direction,

$$u \frac{\partial v}{\partial r} + v \frac{\partial v}{\partial r} = - \frac{1}{\rho} \frac{\partial P}{\partial z} + \frac{1}{r} \frac{\partial}{\partial r} \left(r \varepsilon_r \frac{\partial v}{\partial r} \right) + \frac{\partial}{\partial z} \left(\varepsilon_z \frac{\partial v}{\partial z} \right) \quad . \tag{16}$$

In the above equations, u and v are velocity in the r and z directions, respectively, and the eddy diffusivity tensor is assumed to have components ε_r and ε_z only. With the present state-of-the-art, it is virtually impossible to treat the diffusivities with more detail.

Use of only the ε_r and ε_z components of momentum diffusion is to assume that the diffusion coefficient for v-velocity and u-velocity are the same in a given direction.

Vorticity Transport

In the application of numerical analysis we consider solving Equations (14), (15) and (16) by finite-difference techniques without further simplification. However, we must devise some method to solve for pressure, P. This may be done by taking the divergence of Equations (14) and (15) and adding the results to obtain

$$\nabla 2P = - \left\{ \left(\frac{u}{r} \right)^2 + \left(\frac{\partial u}{\partial r} \right)^2 + \left(\frac{\partial v}{\partial z} \right)^2 + 2 \frac{\partial u}{\partial z} \cdot \frac{\partial v}{\partial r} \right\} \tag{17}$$

where the operator

$$\nabla^2 = \frac{\partial^2}{\partial r^2} + \frac{1}{r} \frac{\partial}{\partial r} + \frac{\partial^2}{\partial z^2}$$

In Equation (17), terms involving derivatives of ε_r and ε_z have been ignored for the sake of this discussion. To obtain a solution to the Coanda dynamics, Equations (15), (16) and (17) would be solved simultaneously. However, experience has shown that Equation (17) is difficult to solve numerically because of required boundary conditions.

To circumvent simultaneous solutions to the pressure equation and associated difficulty with the boundary condition, one may choose to solve an equivalent set of equations which eliminates pressure as an explicit part of the analysis. This approach is called the vorticity transport method.

We define vorticity, ω, as

$$\omega = \frac{\partial u}{\partial z} - \frac{\partial v}{\partial r} \quad . \tag{18}$$

A stream function, ψ, is defined by

$$u = -\frac{1}{r}\frac{\partial \psi}{\partial r} \text{ and} \tag{19}$$

$$v = \frac{1}{r}\frac{\partial \psi}{\partial z} \tag{20}$$

which identically satisfies the continuity Equation (14). An elliptic partial differential equation is obtained for ψ by substituting Equations (19) and (20) into (18) which yields

$$\frac{\partial^2 \psi}{\partial r^2} - \frac{1}{r}\frac{\partial \psi}{\partial r} + \frac{\partial^2 \psi}{\partial z^2} = -r\omega \ . \tag{21}$$

Velocities u and v may be obtained by solving Equation (21) for ψ and then solving the auxiliary Equations (19) and (20).

However, to obtain solution to Equation (21), the flow field vorticity, $\omega(r,z)$, must be known. A vorticity transport equation may be derived by cross-differentiating Equations (15) and (16) and subtracting the latter result from the former to obtain

$$\frac{\partial u\omega}{\partial r} + \frac{\partial v\omega}{\partial z} = \varepsilon_r \frac{\partial}{\partial r}\left(\frac{1}{r}\frac{\partial \omega r}{\partial r}\right) + \varepsilon_z \frac{\partial^2 \omega}{\partial z^2} + \frac{\partial}{\partial z}\left(\frac{1}{r}\frac{\partial ur}{\partial r}\cdot\frac{\partial \varepsilon_r}{\partial r} + \frac{\partial u}{\partial z}\cdot\frac{\partial \varepsilon_z}{\partial z}\right)$$

$$+ \frac{\partial \varepsilon_r}{\partial z}\cdot\frac{\partial}{\partial r}\left(\frac{1}{r}\frac{\partial ur}{\partial r}\right) + \frac{\partial \varepsilon_z}{\partial z}\cdot\frac{\partial^2 u}{\partial z^2} - \frac{\partial}{\partial r}\left(\frac{\partial v}{\partial r}\cdot\frac{\partial \varepsilon_r}{\partial r} + \frac{\partial v}{\partial z}\cdot\frac{\partial \varepsilon_z}{\partial z}\right)$$

$$- \frac{\partial \varepsilon_r}{\partial r}\cdot\left(\frac{\partial^2 v}{\partial r^2} + \frac{1}{r}\frac{\partial v}{\partial r}\right) - \frac{\partial \varepsilon_z}{\partial r}\cdot\frac{\partial^2 v}{\partial z^2} \quad . \tag{22}$$

If the turbulent structure of the flow field is homogeneous and isotropic, derivatives of ε_r and ε_z vanish and the vorticity transport equation becomes

$$\frac{\partial u\omega}{\partial r} + \frac{\partial v\omega}{\partial z} = \varepsilon_0 \frac{\partial}{\partial r}\left(\frac{1}{r}\frac{\partial \omega r}{\partial r}\right) + \varepsilon_0 \frac{\partial^2 \omega}{\partial z^2} \quad . \tag{23}$$

Note that pressure, P, does not explicitly appear in Equations (22) and (23). Once the vorticity solution is obtained (and hence, the velocity solution), one may back-calculate pressure from Equation (17). Alternatively, pressure may also be calculated using either Equation (15) or (16).

Description of the SYMJET Code (Coanda Version)

The Coanda version of the SYMJET code solves Equations (21) and (22) along with the auxiliary relationships Equations (19) and (20), by finite-difference techniques. However, these equations are first scaled with the dimensionless variables and parameters defined as follows:

$$R = r/r_0$$

$$Z = z/r_0 \ , \ \bar{Z} = z/D$$

$$U = u/v_0$$

$$V = v/v_o$$

$$\psi = \psi/\left(r_o^2\ v_o\right)$$

$$\Omega = \omega\ r_o/v_o$$

$$RE_r = \frac{r_o v_o}{\varepsilon_r}\ ,\ \text{(radial, turbulent Reynolds No.)}$$

$$RE_z = \frac{r_o v_o}{\varepsilon_z}\ ,\ \text{(vertical, turbulent Reynolds No.)}$$

In the above, r_o is the characteristic radius of the Coanda eductor and v_o is a characteristic reference velocity which may be taken as the Coanda slot velocity.

In their scaled form the governing equations become:

Stream Function:

$$\frac{\partial^2\Psi}{\partial R^2} - \frac{1}{R}\frac{\partial\Psi}{\partial R} + \frac{\partial^2\Psi}{\partial Z^2} = -\ R\Omega \tag{24}$$

Vorticity Transport:

$$\frac{\partial U\Omega}{\partial R} + \frac{\partial V\Omega}{\partial Z} = \frac{1}{RE_r}\left(\frac{\partial^2\Omega}{\partial R^2} + \frac{1}{R}\frac{\partial\Omega}{\partial R} - \frac{\Omega}{R^2}\right) + \frac{1}{RE_z}\frac{\partial^2\Omega}{\partial Z^2}\ , \tag{25}$$

along with the auxiliary relationships for velocity:

$$U = -\frac{1}{R}\frac{\partial\Psi}{\partial Z} \tag{26}$$

$$V = \frac{1}{R}\frac{\partial\Psi}{\partial R} \tag{27}$$

Terms involving derivatives of RE_r and RE_z are not included in Equation (25) but are accounted for in the SYMJET code.

Finite Difference Grid System

The finite difference grid layout consists of two grid systems. One grid is used to calculate the stream function, Ψ, which provides information to compute velocity components, U and V. This system coincides with the physical boundaries and is illustrated by the wider lines on Figure 6. The stream function is calculated at the system interior intersection points designated by the solid round symbols. The U components of the velocity field are computed at vertical midpoints which are designated by open circle symbols; whereas, the V components are computed at horizontal midpoints (K coordinate) and designated by open box symbols. In this manner, the stream function grid layout defines a system of cells with the stream function, Ψ, computed at each corner point (or set by boundary conditions, as the case may be) and velocities defined at the center of the cell face.

The second grid system is used to calculate vorticity, Ω, and is illustrated in Figure 6 by the narrow lines. This layout completely overlaps the Ψ grid (and physical system) with interior intersection points centered in the cells which are defined by the Ψ grid system. These interior grid points are indicated by crosses.

This staggered grid system is used for computational convenience in treating boundary conditions and to permit direct evaluation of convective transport terms at cell faces.

The Ψ grid system is sized by NJ and NK grid points in the R direction and vertical direction, respectively. The Ω system has size NJ + 1 and NK + 1 in the respective directions. Points on the Ψ grid are indicated by (j, k), whereas points on the Ω grid are specified by (p, q). Vertical spacing for the system is defined by ΔZ_k which may be variable. Grid spacing along the R coordinate is designated by ΔR.

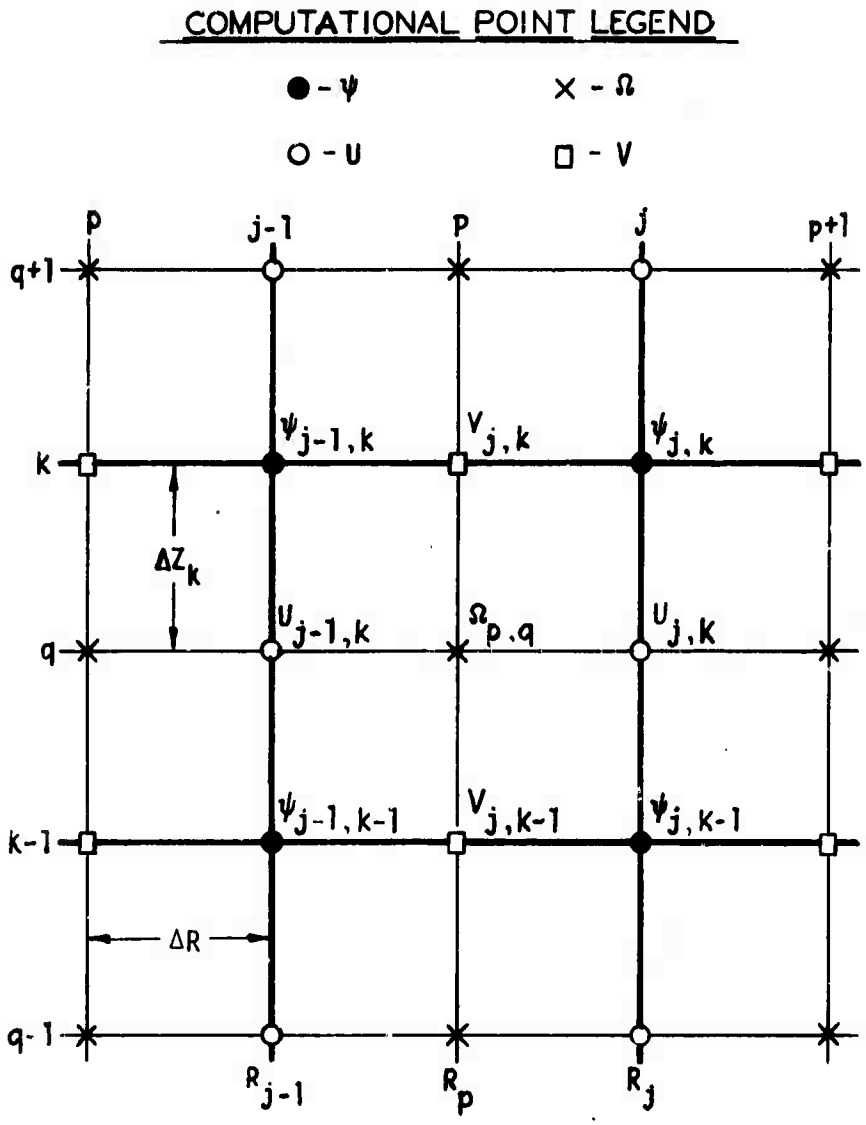

FIGURE 6. Typical Finite Difference Cell Illustrating Indices for ψ, Ω, and V

Difference Equations

Standard difference representation is used wherever possible in this discussion. Central differences are used for both first and second partial derivatives except for convective terms where special upstream methods are used. These methods are similar to those used by Torrance and Rockett[6] and Runchal and Wolfshtein,[7] and details of the application here are explained by Trent [8] Techniques for uneven spacing are used for the vertical differences.

Stream Function and Velocity

Consider the stream function grid system illustrated in Figure 6. The finite difference representation of Equation (24) based on central differences for both first and second partial derivatives is as follows:

$$2\left(\frac{1}{\Delta R^2} + \frac{1}{\Delta Z_k \Delta Z_{k+1}}\right)\Psi_{j,k} = \frac{1}{\Delta R^2}\left(1 - \frac{\Delta R}{2R}\right)\Psi_{j+1,k} + \frac{1}{\Delta R^2}\left(1 + \frac{\Delta R}{2R}\right)\Psi_{j-1,k}$$

$$+ \frac{2}{\Delta Z_{k+1}\left(\Delta Z_{k+1} + \Delta Z_k\right)} \cdot \Psi_{j,k+1}$$

$$+ \frac{2}{\Delta Z_k\left(\Delta Z_{k+1} + \Delta Z_k\right)} \cdot \Psi_{j,k-1} + \overline{\Omega}_{j,k} R_j \quad . \qquad (28)$$

In the above difference equation, the quantity $\overline{\Omega}_{j,k}$ is the average value vorticity at point (j,k), hence the overbar. This average value is used since $\Omega_{p,q}$ does not lie on the Ψ computational grid.

Velocity is calculated at cell faces by

$$U_{j,k} = \frac{-1}{R_j \, \Delta Z_k} \cdot \left(\Psi_{j,k} - \Psi_{j,k-1}\right) \qquad (29)$$

and

$$V_{j,k} = \frac{1}{R_j \, \Delta R} \cdot \left(\Psi_{j,k} - \Psi_{j-1,k} \right) \quad . \tag{30}$$

Transport Equations

Referring to the p,q grid system illustrated in Figure 6, the difference representation of the steady flow vorticity transport Equation (25) is written as (after collecting terms).

$$\left[\frac{2}{RE_z \Delta Z_k} \cdot \left(\frac{1}{\Delta Z_k + \Delta Z_{k+1}} + \frac{1}{\Delta Z_k + \Delta Z_{k-1}} \right) + \frac{1}{RE_r \Delta R^2} \cdot \left(2 + \frac{\Delta R^2}{R^2_p} \right) + \frac{1}{2\Delta R} \cdot \left(|U_{j,k}| \right.\right.$$

$$\left. + U_{j,k} + |U_{j-1,k}| - U_{j-1,k} \right) + \frac{1}{2\Delta Z_k} \cdot \left(|V_{j,k}| + V_{j,k} + |V_{j,k-1}| \right.$$

$$\left.\left. - V_{j,k-1} \right) \right] \Omega_{p,q} = \left[\frac{1}{2\Delta R} \cdot \left(|U_{j-1,k}| + U_{j-1,k} \right) + \frac{1}{RE_r \Delta R^2} \right.$$

$$\left. \cdot \left(1 - \frac{\Delta R}{2R_p} \right) \right] \Omega_{p-1,q} + \left[\frac{1}{2\Delta R} \cdot \left(|U_{j,k}| - U_{j,k} \right) + \frac{1}{RE_r \Delta R^2} \right.$$

$$\left. \cdot \left(1 + \frac{\Delta R}{2R_p} \right) \right] \Omega_{p+1,q} + \left[\frac{1}{2\Delta Z_k} \cdot \left(|V_{j,k-1}| + V_{j,k-1} \right) + \frac{2}{RE_z \Delta Z_k} \right.$$

$$\left. \cdot \left(\frac{1}{\Delta Z_k + \Delta Z_{k-1}} \right) \right] \Omega_{p,q-1} + \left[\frac{1}{2\Delta Z_k} \cdot \left(|V_{j,k}| - V_{j,k} \right) + \frac{2}{RE_z \Delta Z_k} \right.$$

$$\left. \cdot \left(\frac{1}{\Delta Z_k + \Delta Z_{k+1}} \right) \right] \Omega_{p,q+1} \quad . \tag{31}$$

The SYMJET code solves the two difference Equations (28) and (31) by Gauss-Siedel iteration. Iteration is continued until the computed velocity meets a particular convergence criterion. Although this criterion is left to the discretion of the user, computation in the present work was carried out until the maximum relative change in velocity for the entire flow field was less than 10^{-3} for one iteration.

Application of SYMJET Code to Coandá Eductor

The SYMJET computer code is presently being applied to predict detailed flow fields in the Coanda eductor. Initial efforts in applying the code were to develop a routine to permit arbitrary specification of boundary conditions from input. This routine has proven highly successful. At present, all boundary conditions can be easily specified. A search routine built into the program maps the specified points onto the overall grid system.

At present, some success has been achieved in predicting flow fields for realistic cases. Steady state, well-converged solutions have been obtained for several flow situations. The grid system used for these cases is shown in Figure 7. The solid boundaries were selected to closely model an existing, workable, Coanda eductor.

At the center of the nozzle, the boundary condition requires that the velocity gradient in the radial direction be zero. Along the outer walls of the eductor, the no-slip criteria (velocity zero at solid wall) was used. At the outlet, velocity profiles were specified; at the inlet (top of Figure 7), the free-flow boundary condition was used. This condition requires only that the streamlines remain straight as they enter. At the primary jet opening, the velocity was specified.

The unequal grid spacing evident in Figure 7 was required to adequately handle flow issuing from the primary jet. Initial attempts to use an equal spacing, with only a single-mesh node being within the primary jet, failed to converge.

Only the inlet section of the Coanda eductor was included in the calculational grid system. Although it is possible to include downstream

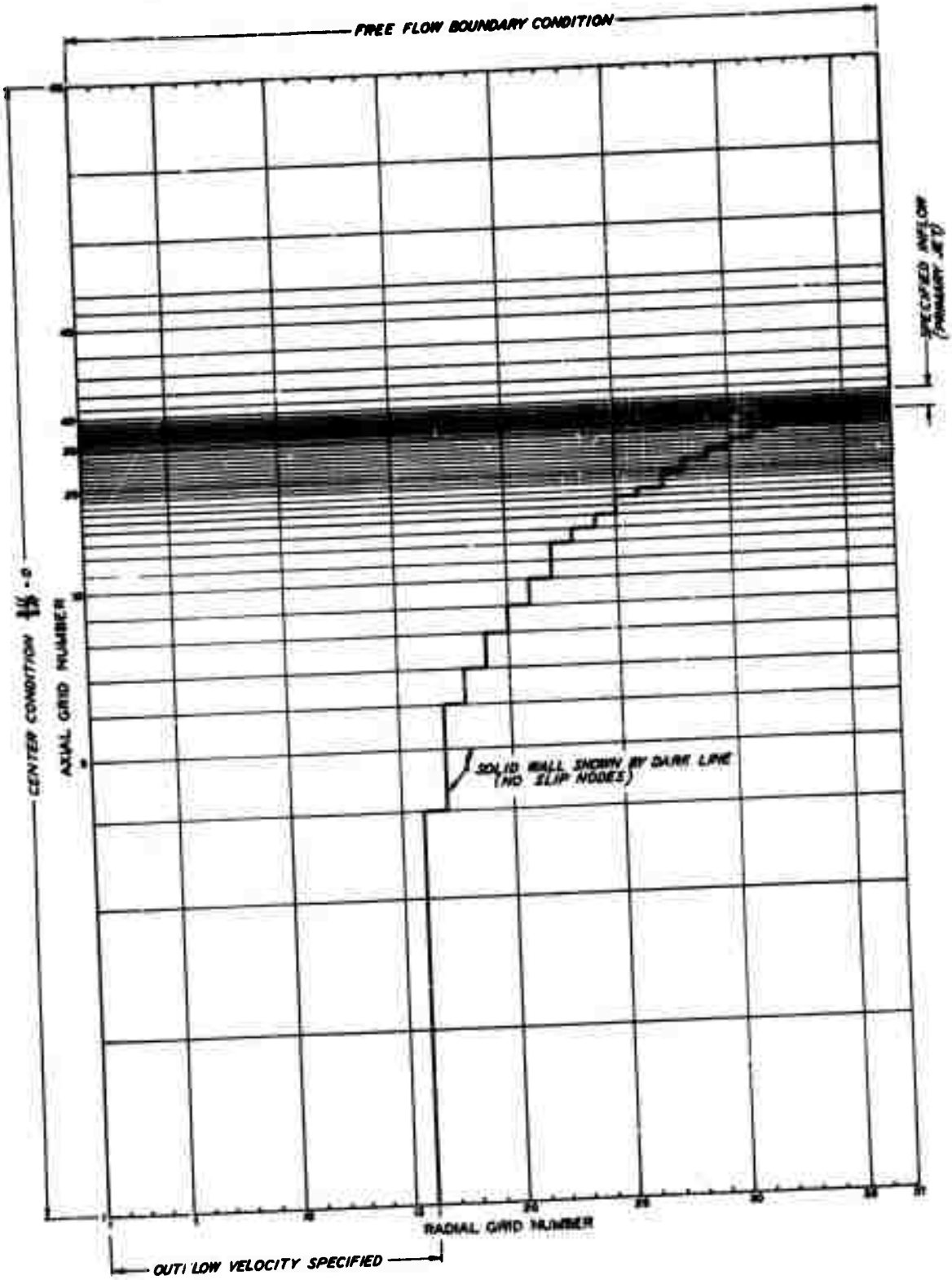

FIGURE 7. Calculational Grid System Showing Boundary Conditions and Grid Spacing

regions, this would substantially increase the number of calculational nodes and the computer time. This was considered unnecessary for initial runs.

Results for a typical case in which the total air flow was five times the flow of the primary air are presented in Figure 8. The shape of the streamlines demonstrates that the primary jet becomes attached to the outer wall of the eductor, and entrains additional air.

Figure 9 shows results obtained for a lower entrainment ratio. The total air flow was reduced by lowering the specified outlet velocity. The total flow leaving through the outlet (bottom of Figure 9) was slightly lower than that entering through the primary air slit. Flow separation occurred near the center of the nozzle, with a part of the primary air exiting through the normal inlet. It is worth noting that this type of behavior could not be predicted using similarity theory because the velocity profiles are not similar at the various downstream positions.

In addition to the streamline output shown in Figures 8 and 9, the SYMJET program prints velocity components, stream functions, and vorticity at each flow node.

For the cases shown in Figures 8 and 9, the eddy viscosity was taken as constant throughout the whole flow field. This is recognized as a gross simplification which will be improved upon as soon as comparative experimental data become available.

Pressure is eliminated as a variable in the vorticity transport method of flow calculation, hence it was not calculated in predictions made to date. Since pressure drop is an important consideration in the operation of an eductor, the next major effort in this work will be devoted to numerical calculation pressure.

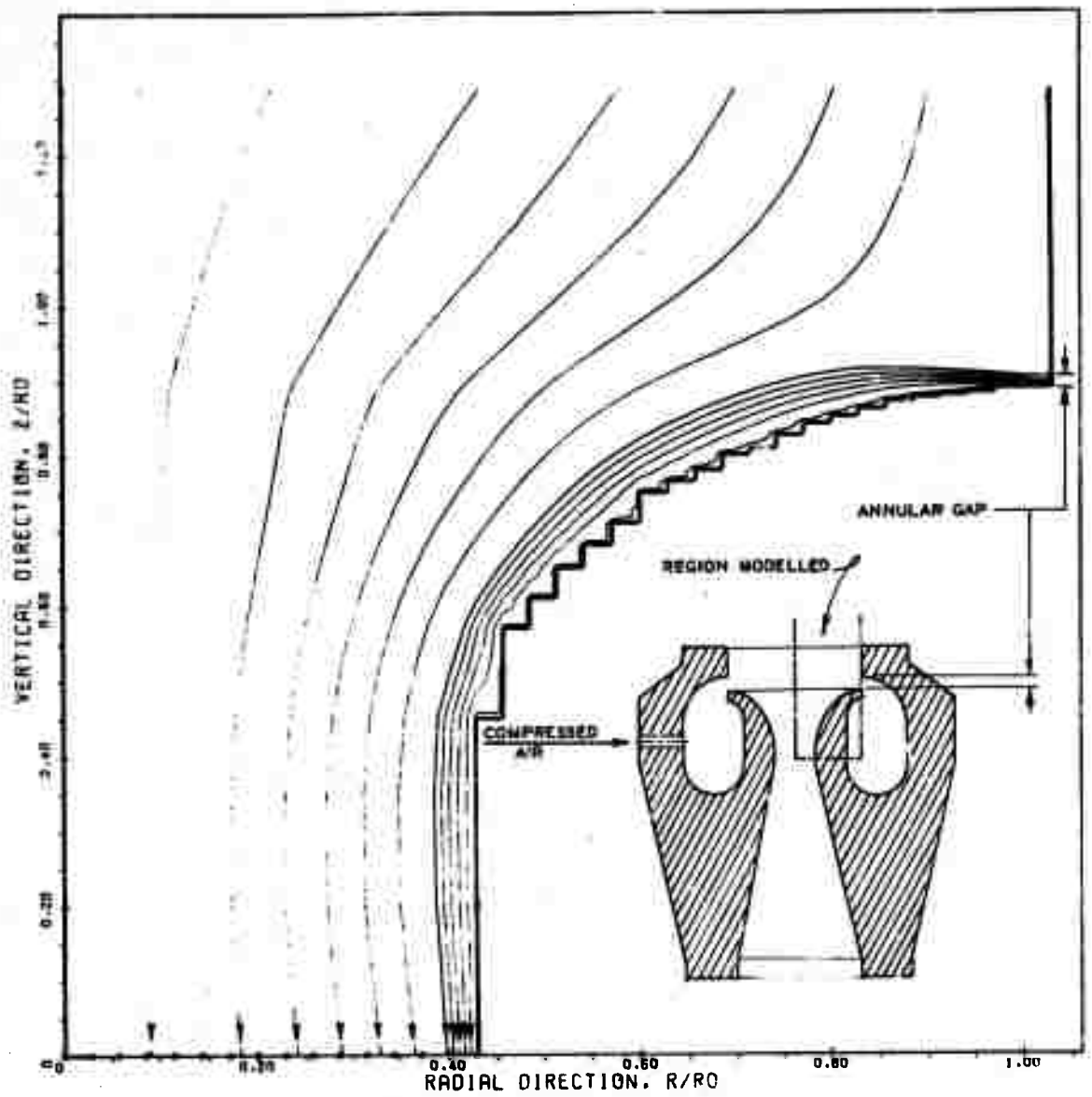

FIGURE 8. Streamlines Predicted for an Entrainment Ratio of 5

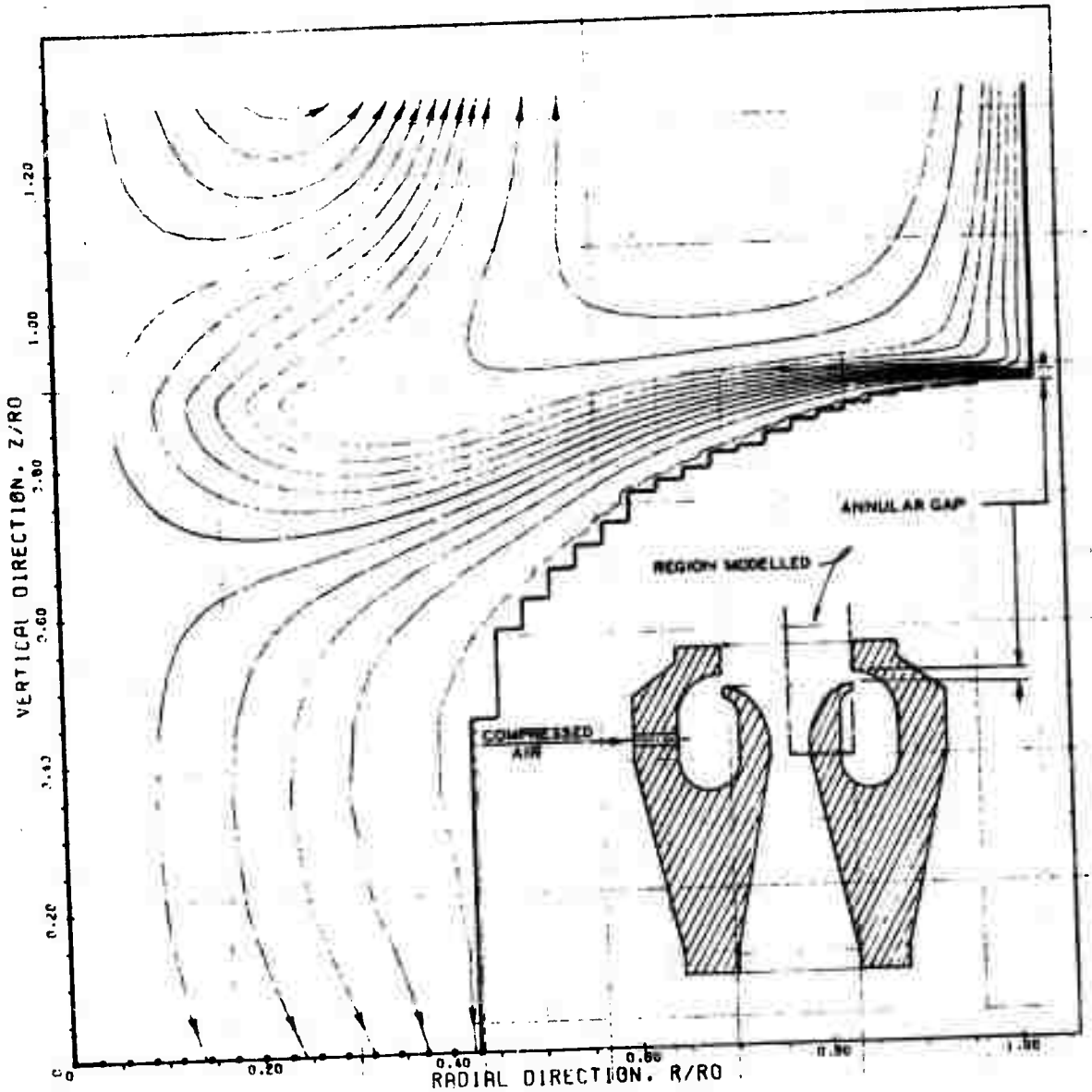

FIGURE 9. Streamlines Predicted for an Entrainment Ratio of 0.8

EXPERIMENTAL PROGRAM

The experimental apparatus is shown in Figure 10. It will be used to gather data on pressure, temperature, air flow and velocity profiles at critical sections of the Coanda eductor. Performance predictions of the analytical program which will be matched by the experimental program are: entrained flow rate to primary jet flow rate, maximum total developed pressure, static pressure difference between eductor inlet and outlet, velocity profiles in the entrainment sections of the eductor, and efficiency of energy interchange of the primary air jet to combined primary-entrained air stream.

The initial experiments required in support of the analytical model will provide data that will allow the determination of turbulent viscosities in the inlet region of a Coanda eductor. This information is essential to obtain realistic predictions because turbulence is expected to play an important role in attachment and detachment of the primary jet and to entrainment of fluid.

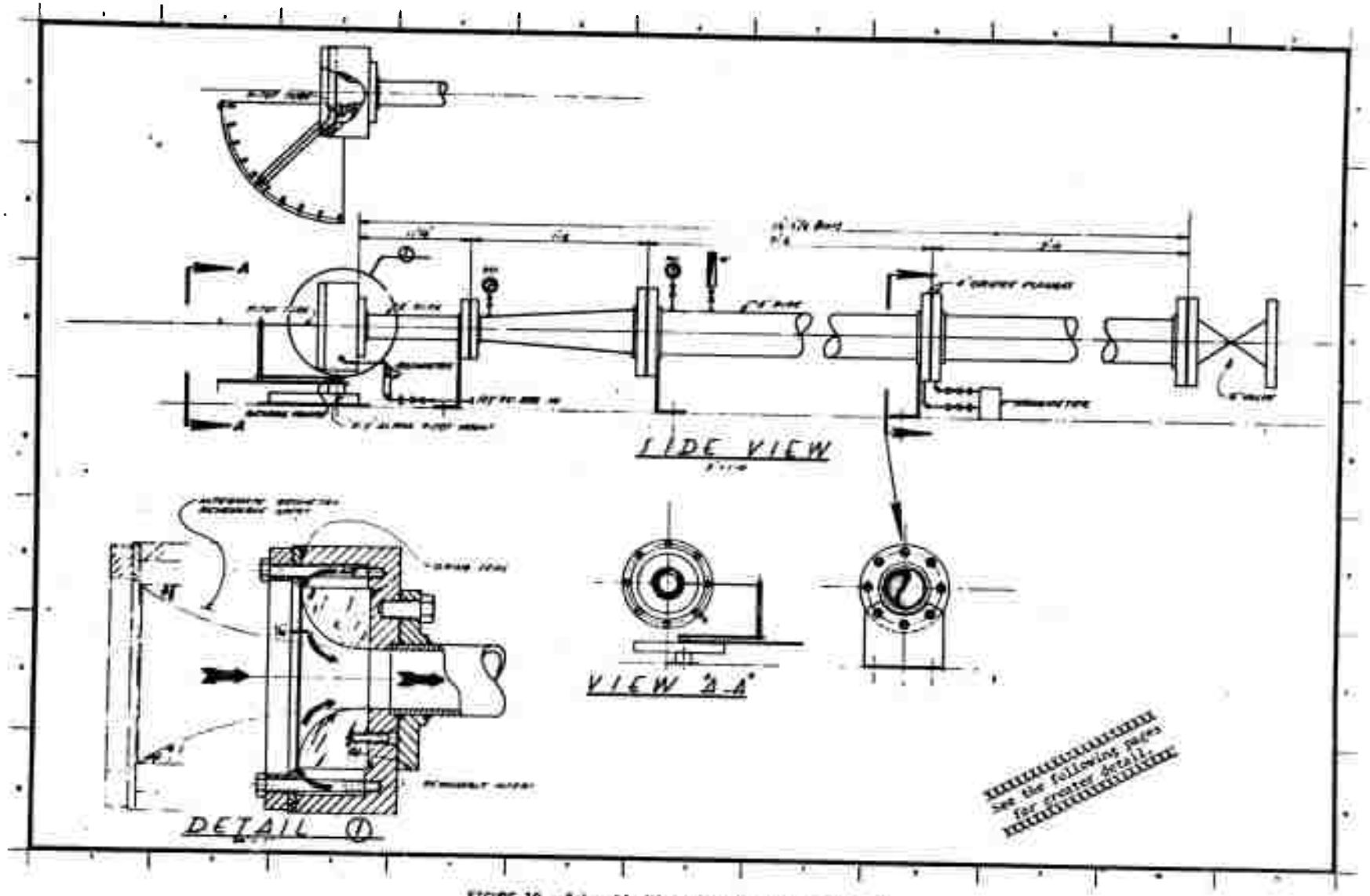

FIGURE 10. Schematic View of Experimental Equipment

36 A

36 B

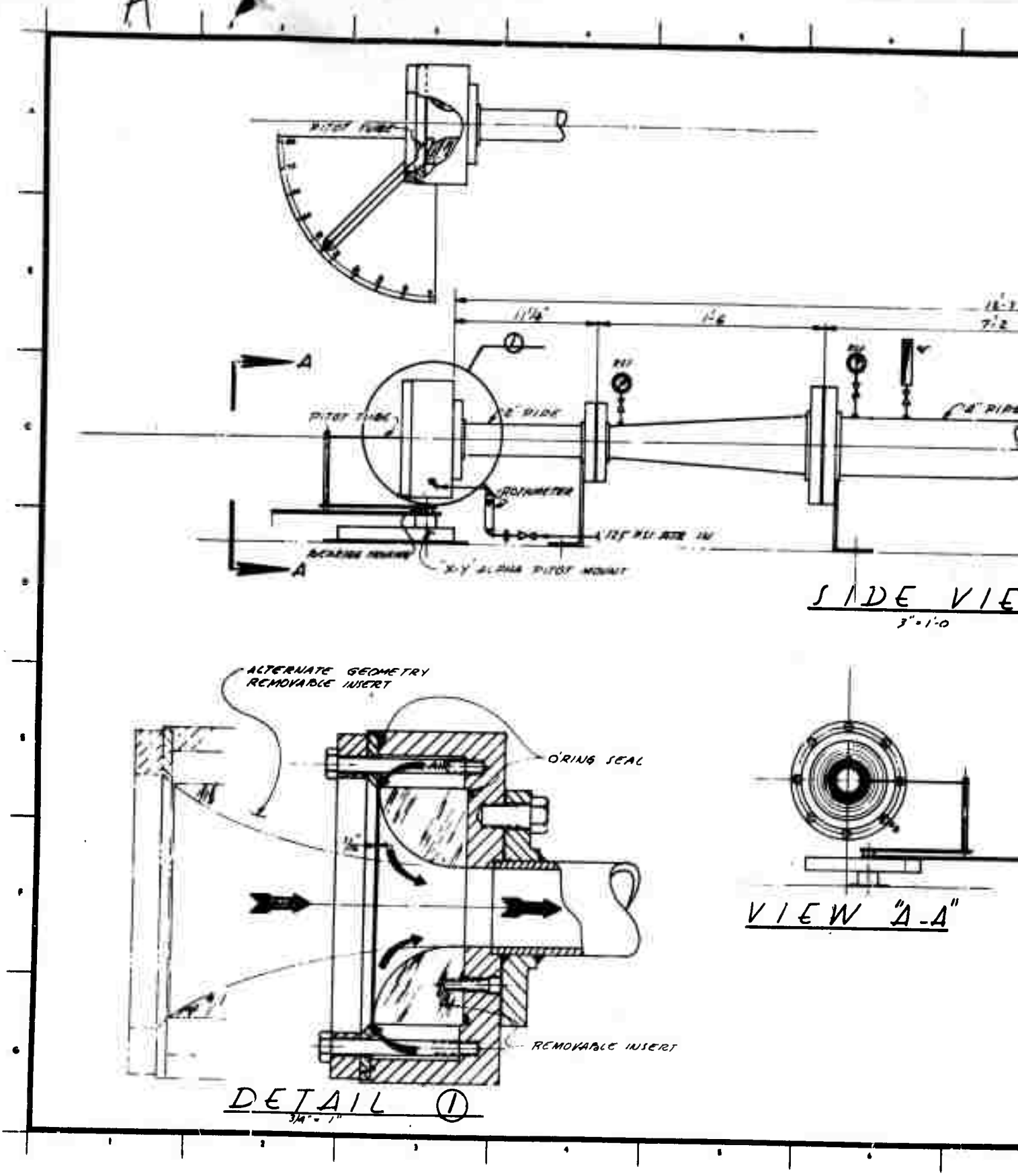

FIGURE 10. Schematic View of Experimenta

36 A

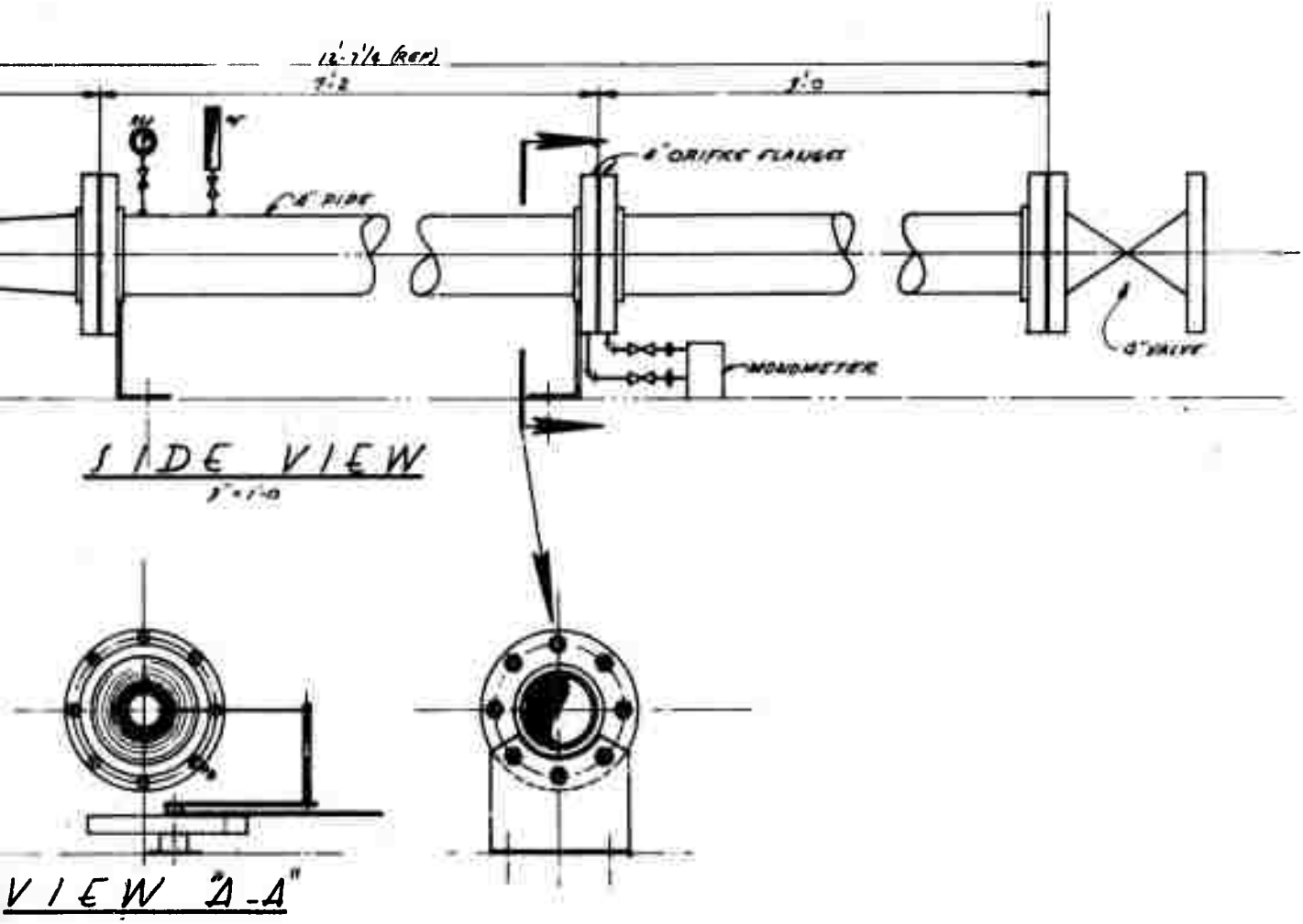

hematic View of Experimental Equipment

36B

REFERENCES

1. C. Bourque and B. G. Newman. "Reattachment of Two-Dimensional, Incompressible Jet to an Adjacent Flat Plate," The Aeronautical Quarterly, Vol. XI, pp. 201-232, August 1960.

2. K. Sridhar and P.K.C. Tu. "Experimental Investigation of Curvature Effects on Turbulent Wall Jets," The Aeronautical Journal of the Royal Aeronautical Society, Vol. 73, pp. 977-981, November 1969.

3. M. B. Glauert. "The Wall Jet," Journal of Fluid Mechanics, Vol. 1, pp. 625-643, 1956.

4. A. Klinkenberg and H. H. Mooy. "Dimensionless Groups in Fluid Friction, Heat and Material Transfer," Chemical Engineering Progress, Vol. 44, No. 1, pp. 17-36, January 1948.

5. J. G. Knudsen and D. L. Katz. Fluid Dynamics and Heat Transfer, McGraw-Hill Book Company, Inc., 1958, pp. 132-133.

6. K. E. Torrance and J. A. Rockett. "Numerical Study of Natural Convection in an Enclosure with Localized Heating from Below-Creeping Flow to the Onset of Laminar Instability," Journal of Fluid Mechanics, Vol. 36, No. 1, pp. 33-54, 1969.

7. A. K. Runchal and M. Wolfshtein. "Numerical Integration Procedure for the Steady-State Navier-Stokes Equations," Journal of Mechanical Engineering Science, Vol. 11, No. 5, pp. 445-453, 1969.

8. D. S. Trent. "A Numerical Model for Predicting Heat Dispension in Thermal Plumes Issuing from Large, Vertical Outfalls in Shallow Coastal Waters," Doctoral Dissertation, Corvallis, Oregon. (To be published.)

APPENDIX A

PROJECT ORGANIZATION CHART

APPENDIX A

PROJECT ORGANIZATION ACCORDING TO FUNCTION

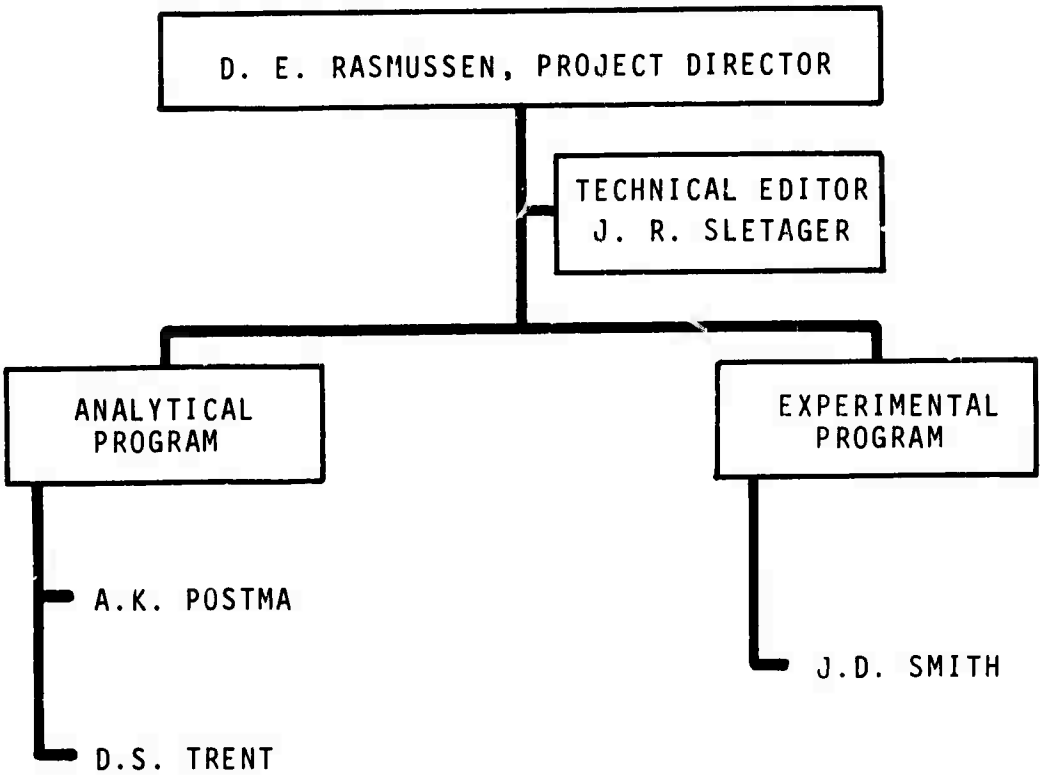

APPENDIX B

BIBLIOGRAPHY OF LITERATURE RELATED TO COANDA EDUCTORS

BIBLIOGRAPHY

Abbott, D.E. and Kline, S.J., "Experimental Investigation of Subsonic Turbulent Flow Over Single and Double Backward Facing Steps", Journal of Basic Engineering, pp. 317-325, Sept. 1962.

Anderson, D.C., Jr., "An Experimental Investigation of Compressible Jet Wall Attachment at Low Reynolds Numbers", 1969, University Microfilm 69-18608.

Bangert, L.H., "The Turbulent Wall Jet with an Initial Boundary Layer", AIAA Paper No. 71-612, June 1971.

Beeken, B.B., "A Theoretical and Experimental Study of a Coanda Curved Wall Attachment Device", ASME, Winter Annual Meeting and Energy Systems Exposition, N.Y., N.Y., Dec. 1-5, 1968, Paper 68-WA/FE-27.

Binion, T.W., Jr., "Investigation of the Recirculation Region of a Flow Field Caused by a Jet in Ground Effect with Crossflow", AEDC-TR-70-192, Arnold Engineering Development Center, Air Force Systems Command, Arnold Air Force Station, Tenn., Sept. 1970.

Bourque, C. and Newman, B.G., "Reattachment of a Two-Dimensional, Incompressible Jet to an Adjacent Flat Plate", The Aeronautical Quarterly, Vol. XI, pp. 201-232, August 1960.

Bourque, C. and Nguyen, H., "The Effect of Back Pressure on the Position of Reattachment of a Jet to an Adjacent Flat Plate", Fourth Cranfield Fluidics Conference, 17th-20th March 1970, Coventry, Paper X2.

Brown, F.T., "A Combined Analytical and Experimental Approach to the Development of Fluid-Jet Amplifiers", Journal of Basic Engineering, pp. 175-184, June 1964.

Burkett, R.J., Chalmers-Dixon, P., Morris, P.J. and Pyle, D.L., "On the Flow of Fluidised Solids Through Orifices", Chemical Engineering Science, Vol. 26, No. 3, pp. 405-418, March 1971.

Chavez, S.P. and Richards, C.G., "A Numerical Study of the Coanda Effect", ASME, Fluidics Conference, Atlanta, GA., June 22-23, 1970, Paper 70-Flcs-12.

Chu, Wen-Hwa, "Generalized Finite-Element Method for Compressible Viscous Flow", AIAA Technical Notes, pp. 2275-2276, Nov. 1971.

Davies, G.S., Mitra, A.K. and Roy, A.N., "Momentum Transfer Studies in Ejectors", I&EC Process Design and Development, Vol. 6, No. 3, pp. 293-299, July 1967.

DeFrate, L.A. and Hoerl, A.E., "Optimum Design of Ejectors Using Digital Computers", Computer Techniques, Chemical Engineering Progress Symposium Series, Vol. 55, No. 21, pp. 43-51.

BIBLIOGRAPHY (contd)

de Vries, G. and Norrie, D.H., "The Application of the Finite-Element Technique to Potential Flow Problems", ASME, Journal of Applied Mechanics, pp. 1-5, June 1970.

Edelman, G.M. and Shapiro, A.H., "Tables for Numerical Solution of Problems in the Mechanics and Thermodynamics of Steady One-Dimensional Gas Flow Without Discontinuities", Design Data, Journal of Applied Mechanics, pp. A-344 - A-351.

Erian, F.F., "Influence of Pressure Gradient on Turbulent Flows with Asymmetric Mean Velocity", Journal of Applied Mechanics, pp. 901-904, Dec. 1969.

Esch, R.E., "Numerical Solution of Transient Viscous Flow Problems", SER, pp. 28-34, Winter 1964.

Exley, J.T. and Brighton, J.A., "Flow Separation and Reattachment in Confined Jet Mixing", ASME, Applied Mechanics and Fluids Engineering Conference, Evanston, Ill., June 16-18, 1969, Paper 69-FE-29.

Felsing, G.W. and Moller, P.S., "Coanda Flow Over a Circular Cylinder with Injection Normal to the Surface", AIAA Journal, Vol. 7, No. 5, pp. 842-846, May 1969.

Foa, J.V., "A Pressure Exchanger for Marine Propulsion", Rensselaer Polytechnic Institute, Technical Report Abstract 700095, pp. 346-352.

Gartshore, I.S. and Newman, B.G., "The Turbulent Wall Jet in an Arbitrary Pressure Gradient", The Aeronautical Quarterly, pp. 25-56, Feb. 1969.

Glauert, M.B., "The Wall Jet", Journal of Fluid Mechanics, Vol. 1, pp. 625-643, 1956.

Goradia, S.H. and Colwell, G.T., "Parametric Study of a Two-Dimensional Turbulent Wall Jet in a Moving Stream with Arbitrary Pressure Gradient", AIAA Journal, Vol. 9, No. 11, pp. 2156-2165, Nov. 1971.

Hoge, H.J., Eichacker, S.S. and Fiske, D.L., "Studies of Jet Compression - I, Apparatus and Methods. Results with Air at Room Temperature", Journal of Basic Engineering, pp. 426-432, Sept. 1959.

Hubbartt, J.E. and Bangert, L.H., "Turbulent Boundary Layer Control by a Wall Jet", AIAA Paper No. 70-107, Jan. 1970.

Johnson, L.D., "Experimental Investigation of Turbulent Jet Attachment to a Convex Wall", Naval Postgraduate School, Monterey, Calif., Sept. 1968, University Microfilm AD 847 579.

Kacker, S.C. and Whitelaw, J.H., "The Turbulence Characteristics of Two-Dimensional Wall-Jet and Wall-Wake Flows", ASME, Winter Annual Meeting, N.Y., N.Y., Nov. 29 - Dec. 3, 1970, Paper 70-WA/APM-35.

Kastner, L.J. and Spooner, J.R., "An Investigation of the Performance and Design of the Air Ejector Employing Low-Pressure Air as the Driving Fluid", pp. 149-159.

Keenan, J.H. and Neumann, E.P., "A Simple Air Ejector", Journal of Applied Mechanics, pp. A-75 - A-81, June 1942.

Keenan, J.H., Neumann, E.P. and Lustwerk, F., "An Investigation of Ejector Design by Analysis and Experiment", Journal of Applied Mechanics, pp. 299-309, Sept. 1950.

Keller, J.B., "Teapot Effect", Journal of Applied Physics, Vol. 28, No. 8, pp. 859-864, August 1957.

Kesler, K.L., "Turbulent Jet Attachment to Convex Walls", Naval Postgraduate School, Monterey, Calif., June 1968, University Microfilm AD 838-963.

Kind, R.J., "Calculation of the Normal-Stress Distribution in a Curved Wall Jet", The Aeronautical Journal of the Royal Aeronautical Society, Vol. 75, pp. 343-348, May 1971.

Korbacher, G.K., "The Coanda Effect at Deflection Surfaces Detached from the Jet Nozzle", Canadian Aeronautics and Space Journal, pp. 1-6, Jan. 1962.

Mallonee, R.C. II and Jacoby, S.L.S., "Plane, Turbulent Compressible Wall Jet With and Without Parallel Free Stream", ASME, Fluids Engineering Conference, Symposium on Unsteady Flow, Philadelphia, PA., May 6-9, 1968, Paper 68-FE-40.

Manian, V.S., McDonald, T.W. and Besant, R.W., "Heat Transfer Measurements in Cylindrical Wall Jets", Int. J. Heat Mass Transfer, Vol. 12, pp. 673-679, Pergamon Press, Great Britian, 1969.

McRee, D.I. and Edwards, J.A., "A Simplified Two-Dimensional Jet Reattachment Model", ASME, Winter Annual Meeting, N.Y., N.Y., Nov. 29-Dec. 3, 1970, Paper 70-WA/Flcs-8.

Mehus, T., "An Experimental Investigation into the Shape of Thrust Augmenting Surfaces in Conjunction with Coanda-Deflected Jet Sheets (Part II)", Institute for Aerospace Studies, University of Toronoto, Jan. 1965.

Metral, Albert and Zerner, Frederic, "The Coanda Effect", a facsimile report reproduced by the USAEC, AEC-TR-3386.

BIBLIOGRAPHY (contd)

Miller, E.B., "The Visualization of Turbulent Flows by Means of Flow Birefringence", Wyle Laboratories Research Staff Report WR 67-12, July 1967.

Newman, B.G., "The Deflexion of Plane Jets by Adjacent Boundaries - Coanda Effect", Boundary Layer and Flow Control, pp. 232-264, Pergamon Press, London.

Olson, R.E., "Spreading Rates of Compressible Two-Dimensional Reattaching Jets Upstream of Reattachment", pp. 139-165.

Panitz, T. and Wasan, D.T., "Flow Attachment to Solid Surfaces: The Coanda Effect", AIChE Journal, Vol. 18, No. 1, pp. 51-57, Jan. 1972.

Paranjpe, S.C. and Sridhar, K., "Effects of an Initial Gap on the Turbulent Jet Flow Over a Curved Wall", The Aeronautical Journal of the Royal Aeronautical Society, Vol. 72, pp. 63-67, Jan. 1968.

Pearson, C.E., "A Computational Method for Viscous Flow Problems", J. Fluid Mech., Vol. 21, Part 4, pp. 611-622, 1965.

Perry, C.C., "Two-Dimensional Jet Attachment", 1967, University Microfilm 67-15672.

Plotkin, A., "The Flow of a Laminar, Incompressible Jet Along a Parabola", Journal of Applied Mechanics, ASME Paper No. 71-APM-MM, 1971.

Reba, Imants, "Applications of the Coanda Effect", Scientific America, Vol. 214, pp. 84-93, 1966.

Reiner, Markus, "The Teapot Effect ... A Problem", Physics Today, pp. 16-20, Sept. 1956.

Rockwell, D.O. and Fiske, P.M., "Jet Reattachment to Walls of Various Shapes", Journal of Basic Engineering, pp. 1-6.

Sarpkaya, Turgut, "FLUERICS, 25. The Deflection of Plane Turbulent Jets by Convex Walls, Part - 1", U.S. Army Materiel Command, Harry Diamond Laboratories, Washington, D.C., Nov. 1968.

Sarpkaya, T., "The Performance Characteristics of Geometrically Similar Bistable Amplifiers", Journal of Basic Engineering, Paper No. 68-WA/FE-18, pp. 1-6.

Sarpkaya, T. and Richardson, D.C., "Turbulent Jet Over an Inclined Wall", Journal of Basic Engineering, pp. 287-293, June 1970.

Sato, Masayosi and Matsuoka, Kenji, "Separation Point of Two-Dimensional Tangential Jet Along Circular-Cylindrical Wall", Osaka Prefecture, University Bulletin, Series A - Engineering and Natural Sciences, Vol. 16, No. 2, pp. 205-212, 1967.

Savkar, S.D., "An Experimental Study of Switching in a Bistable Fluid Amplifier", University Microfilms Limited, High Wycomb, England, 1970.

Schneider, J. and Boccio, J., "Calculation of Turbulent Boundary Layers with Heat Transfer and Pressure Gradient Utilizing a Compressibility Transformation, Part III - Computer Program Manual", NASA Contractor Report NASA CR-1925, Jan. 1972.

Shapiro, A.H. and Hawthorne, W.R., "The Mechanics and Thermodynamics of Steady One-Dimensional Gas Flow", Journal of Applied Mechanics, pp. A-317 - A-336, Dec. 1947.

Sheeran, W.J. and Dosanjh, D.S., "Observations on Jet Flows from a Two-dimensional, Underexpanded, Sonic Nozzle", AIAA Journal, Vol. 6, No. 3, pp. 540-542, March 1968.

Sparrow, E.M. and Yu, H.S., "Local Non-Similarity Thermal Boundary-Layer Solutions", Journal of Heat Transfer, pp. 328-334, Nov. 1971.

Squire, L.C., "A Law of the Wall for Compressible Turbulent Boundary Layers with Air Injection", J. Fluid Mech., Vol. 37, Part 3, pp. 449-456, 1969.

Sridhar, K. and Tu, P.K.C., "Experimental Investigation of Curvature Effects on Turbulent Wall Jets", The Aeronautical Journal of the Royal Aeronautical Society, Vol. 73, pp. 977-981, Nov. 1969.

Torda, T.P., Ghia, K.N. and Victory, E.L., "Analysis of Entrainment and Flow Augmentation for Coanda-Type Nozzles", Symposium on the Coanda Effect and Some Special Applications of Aero-Hydrodynamics, Bucharest, Rumania, June 1967, pp. 533-587.

Wei, M.H.Y. and Corsiglia, V.R., "An Analysis of Coanda Jet Flows", NASA SP-228, Analytic Methods in Aircraft Aerodynamics - A Symposium Held at Ames Research Center - Moffett Field, CA., Oct. 28-30, 1969, pp. 197-213.

Wille, R. and Fernholz, H., "Report on the First European Mechanics Colloquium on the Coanda Effect", J. Fluid Mech., Vol. 23, Part 4, pp. 801-819, 1965.

Wygnanski, I.J. and Champagne, F.H., "The Laminar Wall-Jet Over a Curved Surface", J. Fluid Mech., Vol. 31, Part 3, pp. 459-465, 1968.